JOURNAL REVIEW

Modeling Crystal Shapes of Organic Materials Grown from Solution

Daniel Winn and Michael F. Doherty
Dept. of Chemical Engineering, University of Massachusetts, Amherst, MA 01003

The shape of a crystalline organic solid has a major impact on its downstream processing and on its end-product quality, issues that are becoming increasingly important in the specialty and fine chemical, as well as the pharmaceutical and life science, industries. Though it is widely known that improved crystal shapes can be achieved by varying the conditions of crystallization (such as solvent type and impurity levels), there is far less understanding of how to effect such a change. Until recently, most methods for predicting crystal shapes were based exclusively on the internal crystal structure, and hence could not account for solvent or impurity effects. New approaches, however, offer the possibility of accurately predicting the effects of solvents. Models for predicting crystal shape are reviewed, as well as their utility for process and product design.

Introduction

In the chemical process industries, numerous organic materials are purified by solid-liquid separation (such as adipic acid, ibuprofen, and bisphenol A). Many of them, in particular specialty chemicals such as pharmaceuticals, are crystallized from solution. As with other separation techniques, the product purity is the primary measure of product quality. However, unlike other separations, solution crystallization produces materials with specific crystal shapes and size distributions, variables that have a substantial impact on downstream processing and product performance.

The effects of crystal size and shape on solids processes are far reaching. They influence the rate at which material can be processed (such as filtering, washing, and drying), as well as physical properties such as bulk density, mechanical strength, and wettability. Storage and handling characteristics, the ease with which solids flow, and the extent of dust formation are all, to some extent, a function of crystal morphology; so is the dispersibility and stability of crystals in suspension, which is important for materials, such as pigments, that are eventually formulated as colloids.

Crystal morphology also plays a role in the quality and efficacy of solid dose pharmaceuticals. Crystals of different shapes have different *bioavailabilities* (rate and extent of adsorption in the human body—this is often determined by the dissolution rates of different crystal faces), in which case shape must be controlled for both medical and regulatory purposes (Romero et al., 1991). Crystal morphology also affects the ease with which the drug is compressed into tablets (Gordon and Amin, 1984). Both are key factors in the process efficiency and product quality of pharmaceuticals (York, 1983).

The significant impact that crystal size and shape have on crystallization processes requires that they, along with product purity, be tightly controlled. To handle composition and size distribution, there is a plethora of modeling and design techniques (Tavare, 1995; Bermingham et al., 2000). The phase behavior that dictates composition, and the kinetics and mathematics that describe size distribution, are well developed aspects of chemical engineering. On the other hand, the impact of the crystal's growth environment on its final shape is not as well understood (Myerson and Ginde, 1993). This environment may include process effects such as fluid shear, mechanical abrasion from vessels and impellers, and heat and mass transfer. It also includes physico-chemical effects from interactions between crystal surfaces and the ambient phase (often a solution). While they all act in concert, the solution-surface interactions are critical for modeling crystal shape.

Recently, there has been increased interest in the design of solid processes for organic materials, and a corresponding demand for a comprehensive model to predict crystal shape (Davey, 1991; Tanguy and Marchal, 1996). Improved shapes yield an economic benefit that has been demonstrated in in-

Correspondence concerning this article should be addressed to M. F. Doherty.

dustrial situations, for example, in the production of solid dose pharmaceuticals. The Upjohn Company has patented an improvement of their ibuprofen process, where they have changed solvents and obtained shapes that have better filtering, washing, and drying performance, as well as improved tablet formation characteristics (Gordon and Amin, 1984). The result is a substantial reduction in production downtime and better product quality.

In order to improve the design of solids processes, it would be beneficial to include crystal shape prediction in the overall process design and optimization. There are now several practical modeling techniques that are available to the process engineer. In the following sections, we will review the major developments in the field, and introduce the classical theories and the common procedures for calculating crystal shape. These classical approaches are important first steps in morphological analysis, despite the fact that they fail to account for several key factors of industrial solution crystallization—primarily the effect of solvent on crystal shape. In the final section, we will discuss more recent approaches to the problem that promise to overcome these limitations.

Background

The shape of a crystal is determined by the relative rates of deposition of material on various crystal faces. The general rule is that the slower a face grows, the larger its relative size on the crystal. Given enough time, and appropriate conditions, the crystal should evolve into its equilibrium shape, one that minimizes its total surface free energy per unit volume (Gibbs, 1928). In practice, however, such conditions are rarely achieved, and the shape remains in its nonequilibrium growth form.

The overall rate at which the material crystallizes depends on the thermodynamic driving force. If there are no transport limitations, this driving force is simply the supersaturation of the system (Myerson and Ginde, 1993). However, *where* this material is deposited, and at what relative rates, depends on the nature of its incorporation and binding at different crystal faces (Berkovitch-Yellin, 1985a). If these properties were isotropic, the resulting crystal would be spherical. Since, for organic solids, these properties are highly anisotropic (Gibbs, 1928), the crystals are generally nonspherical, with distinct facets of differing surface areas and orientations.

Early observers suggested a relationship between the facet growth properties and the internal crystal structure. As far back as 1849, Bravais (1866) noted that, for a given substance, certain crystal faces almost always appeared, and some of them were almost more prominent (had larger area) than others. He suggested that this was due to the existence of structural *motifs*-surface architectures—that were different on different crystal faces. Faces with motifs that have high molecular densities should be more energetically stable, and grow more slowly, than ones with low molecular densities.

With the advent of X-ray crystallography, anisotropy of crystal packing was confirmed, and substantial effort was devoted to relating internal crystal structure to external crystal shape. Freidel (1907), and later Donnay and Harker (1937), refined the observations of Bravais. Their model, which is often termed the *BFDH model*, predicts the growth rates of faces from a knowledge of a substance's lattice geometry (unit cell dimensions and positions of molecules). It assumes that the most energetically stable, and slowest growing faces are the ones with the highest density of material and the largest spacing between adjacent layers of material.

Hartman and Perdok (1955) expanded on this concept. They suggested that lattice geometry is not an accurate enough measure of internal crystal forces. The actual number and magnitude of intermolecular interactions are more precise measures of face stability and growth rate. In particular, they proposed that a face's growth rate is directly proportional to the interaction energy between a molecule on the face and those in the underlying bulk of the crystal—the molecule's *attachment energy*. Computer implementations of both the attachment energy and the BFDH approaches have been developed, and their predictions have been compared extensively to experimental results (Saska and Myerson, 1983; Berkovitch-Yellin, 1985; Clydesdale et al., 1991). These methods closely predict the shapes of vapor grown crystals; however, since they cannot account for forces external to the crystal structure, they are not accurate for solution growth.

The need to account for external factors in predicting crystal shape was also recognized very early on (Bravais, 1866). However, the first to present a comprehensive study of the effects of growth conditions on organic crystal shapes was Wells (1946). He distinguished two main factors that influence crystal shape: the overall rate of growth, and the external interactions of the crystal with molecules of another kind, that is, solvent and/or impurities. Wells emphasized the similarity between solvent and impurities; both are nonsolutes that influence the rate at which the solute incorporates at crystal faces. He was wary of any proposed mechanisms for modeling crystal-impurity interactions that could not logically be extended to handle crystal-solvent interactions.

Since Wells, many researchers have suggested that impurities and/or solvents affect crystal shape by their preferential adsorption on different crystal faces. It is thought that this ''binding'' reduces the growth rates of certain crystal faces and, hence, modifies the shape. Myerson and Saska (1990) have used the solvent accessible areas of the molecules on crystal faces as a measure of solvent binding. More recently, Walker and Roberts (1993) employed molecular dynamics to calculate the binding energy between solvent and crystal faces. Berkovitch-Yellin (1985) and Berkovitch-Yellin et al. (1985) have developed a technique to estimate the effect of impurity binding. This approach, termed the *tailor-made additive* approach, assumes that a structurally similar additive molecule can substitute for a solute molecule on some crystal faces. It has been applied to a variety of crystal systems (Lahav and Leiserowitz, 1993; Clydesdale et al., 1994; Koolman and Rousseau, 1996).

The goal of these techniques has been to calculate a binding energy of a solvent or impurity and to incorporate this value into the attachment energy model. It is thought that the magnitude of the binding energy is related to an effective reduction in the attachment energy, and, hence, growth rate, of a crystal face. Though this assumption has been shown to be qualitatively correct—a large binding energy generally corresponds to a high likelihood that a face's growth rate will be affected—it has not been adequate for quantitative predictions. Binding energies have yet to be successfully correlated to experimentally grown crystal shapes.

The main drawback of these approaches is their *ad hoc* nature. They stem from the attachment energy model which is difficult to modify to account for process conditions, because it is not based on strict thermodynamic principles or a detailed kinetic model. The binding energies themselves are not well defined properties from a classical physical-chemical point of view. These characteristics are the main impediments towards the improvement and widespread use of these techniques.

Morphological models using more detailed kinetic descriptions of crystal growth have been explored and refined since the 1930s. Volmer, Stranski and others (Volmer and Marder, 1931; Kaichew and Stranski, 1934) developed a *2-D nucleation model* of crystal growth based on the fundamental physics of interface structure and of elementary growth processes. (See also the review by Ohara and Reid (1973).) Burton et al. (1951) proposed a growth mechanism resulting from dislocations on crystal faces (the *BCF model*). Both models address the subtle problem of how facetted (planar) surfaces form on crystals. It is thought that facets occur as a result of layer-by-layer processes: in the 2-D nucleation model, a new layer is initiated by the birth of a 2-D nucleus; in the BCF model, a dislocation on a face forms a spiral that rotates as it grows, and forms a new layer upon each rotation. In addition, the kinetic theory defines conditions under which nonfacetted growth occurs (Burton et al., 1951; Jackson, 1958); that is, conditions where layer-by-layer mechanisms break down, facets become *roughened*, and growth occurs due to the random attachment of molecules onto crystal surfaces. Experiments strongly support the existence of 2-D nucleated, BCF, and roughened growth for different materials and conditions of crystallization (Lewis, 1974; Jetten et al., 1984; Land et al., 1996).

Despite the acceptance of these physical models, they have not been widely employed for predicting crystal shapes. Their application requires kinetic and transport coefficients that depend on both the direction of crystal growth (the orientation of the face) and on the type of solution environment (primarily the solvent). While such parameters can be extracted from experiments that measure face-specific growth rates (Davey et al., 1986), this is not a preferred approach for morphological modeling—one would like to predict crystal shape *a priori*, without having to perform experiments. The use of detailed kinetic models for morphological prediction has been limited mostly to computer studies of simple, idealized systems (Gilmer and Bennema, 1972; Swendson et al., 1976).

Recently, however, the group of Bennema and co-workers (Liu et al., 1995; Liu and Bennema, 1996a,b,c) have re-focused attention on detailed crystal growth kinetics as a means of predicting crystal morphology grown from solution. They have simplified the kinetic models to retain only one solvent dependent parameter, and, furthermore, they have demonstrated that this property can be derived from molecular dynamics simulations of the solution-crystal interface. We have also developed a similar approach (Winn and Doherty, 1998), although one that does not require fluid-phase molecular simulations. It uses only known physical properties of the pure solvent, along with the results of standard attachment energy calculations to estimate face-specific kinetic parameters. These implementations of detailed crystallization kinetics offer the possibility to predict crystal shape under realistic processing conditions.

Equilibrium and Growth Shapes

The equilibrium criterion for the dividing surface between solid and fluid phases was developed by Gibbs (1928). For the case where the solid is a convex body (a crystal), it states that the total surface free energy must be at a minimum for a fixed volume of solid

$$\min \int \gamma(n)\, dS \tag{1}$$

where dS is a differential area of the surface, and γ is the specific surface free energy. The value of γ on any portion of the surface is a function of its orientation, which is defined by n, a unit vector normal to the tangent plane to the surface. If a surface consists entirely of facets, as is often the case with crystals, then the criterion becomes

$$\min \sum_i \gamma(n_i)\, A(n_i) \tag{2}$$

where $A(n_i)$ is the area of a facet of orientation n_i. (Note: each n_i will be referred to as a *facetted direction*.)

The geometric features of the crystal shape that minimizes surface free energy were developed by Wulff (1901). His theorem states that within the equilibrium crystal there is a point, the *Wulff point*, such that the perpendicular distance l from any surface tangent plane of orientation n to the Wulff point is proportional to $\gamma(n)$; that is

$$\frac{\gamma(n_1)}{l_1} = \frac{\gamma(n_2)}{l_2} = \cdots = \frac{\gamma(n_i)}{l_i} \tag{3}$$

Thus, all tangent planes to the crystal are perpendicular to a set of vectors, emanating from the Wulff point (the origin), with direction n and magnitude proportional to $\gamma(n)$. (The proportionality depends on the fixed volume of the crystal.) The equilibrium, or Wulff, shape consists of all points x on the convex envelope of this family of planes

$$\{x : x \cdot n \propto \gamma(n)\} \tag{4}$$

The equilibrium shape is determined by the features of the vector field γn. The end points of these vectors can be plotted, forming a surface termed the polar plot of γ. Properties of the polar plot have been widely studied, because they not only determine the equilibrium shape, but also the stability of the minimizing surfaces with regard to fluctuations. (A complete survey of the properties of the polar plot of surface free energy can be found in the work of Herring (1951, 1953).) Its most important feature is that it exhibits ''cusped'' minima in directions which correspond to facetted directions on the equilibrium crystal. Thus, for completely facetted equilibrium crystals, the Wulff shape can be constructed knowing only discrete values of γ for the facetted directions.

The shape itself has two very important and well known characteristics. Its primary feature is that it scales with volume; that is to say, the ratio of surface-to-origin distances for

any two points on the surface is the same at any volume. The other property applies only to completely facetted Wulff shapes: *the relative area of a facet increases with decreasing* γ.

There are several proofs of Wulff's theorem in the literature, and there is a detailed discussion in the article by Herring (1953). Most begin with the assumption that the Wulff shape is completely facetted. Taylor (1978) developed a rigorous proof for Wulff's theorem for the general case where $\gamma(n)$ takes on any functional form. The proof places the theorem in a general mathematical framework: for any function of the form $F(n)$, there is a convex shape, the *Wulff of F*, that has the least surface integral for a fixed volume.

Although the theoretical equilibrium shape has been widely studied, it has been known for some time that most crystalline materials are not in their equilibrium habit (Gibbs, 1928; Herring, 1953; Hartman, 1963). The vast majority of single crystals, particularly organics, are highly facetted and dominated by one or two forms (symmetry related faces). For these forms to be equilibrium crystals, they would have to be capable of adjusting to small fluctuations in the surroundings. This might require the addition or removal of small amounts of material, while at the same time maintaining the equilibrium shape. However, large facets cannot exchange infinitesimal amounts of material and still be surface energy minimizing: they must exchange whole layers. Hence, crystals develop morphologies that are generally not surface energy minimizing, but are a function of the kinetic processes that control layer growth. (The morphologies are, however, likely to contain most low γ faces. Faces of small γ have small local supersaturation (Gibbs, 1928), and, thus, small driving forces and slow growth rate.) They are commonly referred to as *growth shapes*.

Most kinetic theories of crystal growth suggest that material is added to facets such that each facet grows with a velocity in the direction normal to its plane. For example, Frank (1958) showed by the theory of kinematic waves that the process of layer growth by step propagation resulted in an instantaneous velocity $v(n)$ for each point on the surface in the direction of the surface normal n. Given continuous or discrete values for $v(n)$, Frank deduced a construction for the growth shape at time t: his construction is in fact equivalent to performing a Wulff construction on $v(n)t$.

Recently, Cahn et al. (1991), and Taylor et al. (1992) put this result in a more general mathematical framework. They showed that Frank's construction stems from the solution to a PDE which describes a moving interface. They define a crystal surface as a set of points, each one reaching a position x in time t. If there is a point x with surface normal n on an initial surface, and, after a time δt, there is a point $x + \delta x$ with the same surface normal n on a new surface, then dx/dt is the velocity of points of constant n. Each point on the surface also has an instantaneous velocity $v(n)$ in the direction n. This is assumed to be a known quantity, estimated from mechanistic models and physical properties. Thus, the relationship

$$\frac{dx}{dt} \cdot n = v(n) \tag{5}$$

If we define an arrival time, $\tau(x)$, as the time for a point on the surface to reach x, then $\tau(x) = t$ is an implicit equation for the shape of the crystal (for the set of all x on the surface). That is to say, $\tau(x) = t_1$ is the shape at t_1, $\tau(x) = t_2$ is the shape at t_2, and so on, as illustrated in Figure 1.

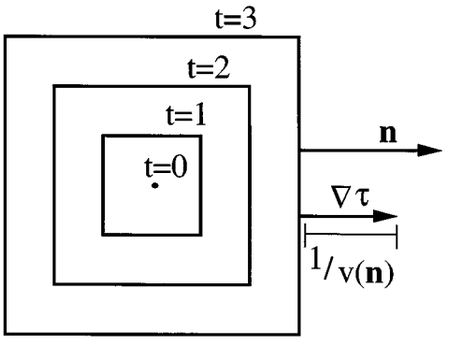

Figure 1. Two-dimensional representation of an evolving cubic crystal.

t represents time, τ is the arrival time n is the unit normal vector, and v is the velocity of the face.

Differentiating $\tau(x)$ and applying the chain rule

$$\frac{d\tau}{dt} = 1 = \nabla\tau \cdot \frac{dx}{dt} \tag{6}$$

and comparing this with Eq. 5, we see that $\nabla\tau$ is a vector with a magnitude of 1/v, and a direction coincident with n, the surface normal. This is the well known result in differential geometry for the motion of a surface tracked by "level sets" of a function (see Taylor et al., 1992). The gradient of τ is also defined by Frank (1972) as the *slowness vector* of a surface. Thus, the equation of motion of the surface is expressed as

$$|\nabla\tau| v(n) - 1 = 0 \tag{7}$$

where $|\nabla\tau|$ is the Euclidean length of vector $\nabla\tau$.

Since $v(n)$ is a function only of direction, it is a first-order homogeneous function. It can be extended on all vectors p, where $p = pn$, so that $v(p) = pv(n)$. Thus $|\nabla\tau| v(n) = v(|\nabla\tau| n)$, and Eq. 7 becomes

$$v(\nabla\tau) - 1 = 0 \tag{8}$$

which is an implicit PDE for the motion of the surface.

This equation has the general form $F(x, \tau, p) = 0$, where $p = \nabla\tau$. Under conditions of smoothness in F, this initial-value problem has an analytical solution by the *method of characteristics* (John, 1975); we expect the solution to be of the form $\tau(x, p)$. In this method, curves parameterized by some variable s, defined as $x(s)$, and termed characteristics, emanate from every point x_0 on the initial surface. They are determined by the following set of ordinary differential equations

$$dx/ds = \nabla_p F(x, \tau, p) \tag{9}$$

$$d\tau/ds = p \cdot \nabla_p F(x, \tau, p) \tag{10}$$

$$dp/ds = -\nabla_x F - p\frac{\partial F}{\partial \tau} \tag{11}$$

where $\nabla p = \partial/\partial p_i$ for $i = 1, 2, 3$.

It is readily shown that $p \cdot \nabla_p F = \mathrm{v}(p) = 1$, and hence $d\tau/ds = 1$; the parameter s is just the arrival time. Also, in the case where v is not an explicit function of x or t, as is true for the conventional problem of the kinetic growth of organic crystals, Eq. 11 reduces to $dp/dt = 0$. Therefore, p and n are constant along characteristics, which are, from Eq. 9, just the straight line trajectories of points of constant n

$$\frac{dx}{dt} = \nabla_p \mathrm{v}(p) \tag{12}$$

$$x = x_0 + t\nabla_p \mathrm{v}(p) \tag{13}$$

The construction of the crystal surface can be further clarified by expanding $\nabla_p \mathrm{v}(p)$

$$\begin{aligned} d\mathrm{v}(p) &= \nabla_p \mathrm{v}(p) \cdot dp \\ &= \nabla_p \mathrm{v}(p) \cdot (\mathrm{p}\,dn + n\,\mathrm{dp}) \end{aligned}$$

Comparing it to

$$d\mathrm{v}(p) = \mathrm{p}\,\mathrm{dv}(n) + \mathrm{v}(n)\mathrm{dp}$$

we see that the gradient of $\mathrm{v}(p)$ has the following properties

$$\nabla_p \mathrm{v}(p) \cdot n = \mathrm{v}(n) \tag{14}$$

$$\nabla_p \mathrm{v}(p) \cdot dn = \mathrm{dv}(n) \tag{15}$$

The vector dn lies in a plane perpendicular to n and hence, it is tangential to the crystal surface. It equals $d\theta T$, where T is the tangent vector to the crystal surface in the direction of maximum increase of v with n, and $d\theta$ is the magnitude of angular change in n (Hoffman and Cahn, 1972). Equation 13 can therefore be rewritten as the sum of normal and tangential components

$$\frac{x - x_0}{t} = \mathrm{v}n + \left(\frac{\partial \mathrm{v}}{\partial \theta}\right)_{\max} T \tag{16}$$

where v refers to $\mathrm{v}(n)$. This expression completely determines the position of all points on the surface.

Facetted portions of a surface are those where x is multivalued; that is, to say, where there are many x with the same surface normal n. This requires having multiple characteristics for a single n. From Eq. 16, we see that multiple characteristics must all have the same normal component, and hence, must all have different tangential components. This occurs when $\partial \mathrm{v}/\partial\theta$ is undefined, as is the case when there is a discontinuity, a ''cusp,'' in the polar plot of $\mathrm{v}(n)$. The magnitude of the tangential components are in a range bounded by the limiting values of $\partial \mathrm{v}/\partial\theta$ as the discontinuity is approached from both sides (positive and negative T). The multiple trajectories that emanate from points on facets are termed *fans* of characteristics. Physically speaking, they are a result of the fact that a point on a facet n at t_1 could follow numerous trajectories and still arrive on facet n of the new surface at t_2.

It we start the crystal growth process from a single point, an origin, then all characteristics x defined by Eq. 16 emanate from that point. For nonfacetted directions, Eq. 16 yields one characteristic, while for facetted n, it yields *fans* of x with the same normal components: $x \cdot n = \mathrm{v}(n)t$. The locus of all x is the crystal surface.

If two or more characteristics intersect—as happens when a characteristic from one fan (of a given facet) crosses a characteristic stemming from another fan (of another facet)—they cannot be included in the crystal surface. A crystal surface by definition must be continuous, and the end points of intersecting characteristics do not form part of a continuous locus. These intersections are termed *shocks*, and correspond to edges and corners in the crystal.

The occurrence of *fans* and *shocks* in the solution of the PDE results in a unique construction for the case of a completely facetted crystal growing from an origin. It has a surface defined by all the characteristics of Eq. 16, minus those cut off by shocks, with all characteristics grouped into sets of x such that $x \cdot n = \mathrm{v}(x)\mathrm{t}$. In other words, it is the envelope of the family of planes defined by

$$\{x : x \cdot n = \mathrm{v}(n)t\} \tag{17}$$

This envelope of planes is clearly equivalent to the envelope of planes described by Eq. 4. Therefore, the construction of a growth crystal at time t, given a function $\mathrm{v}(n)$, is equivalent to the construction of the Wulff of $\mathrm{v}(n)\mathrm{t}$.

This result can also be inferred from the work of Hoffman and Cahn (1972), who showed that $\nabla\gamma(p)$ is a vector field whose locus of tips encloses the Wulff of $\gamma(n)$. Hence, the vector field $\nabla \mathrm{v}(p)$ which defines the *characteristics* of the PDE, also defines the Wulff of $\mathrm{v}(n)$. The Wulff of $\mathrm{v}(n)$ is thus the relative growth shape of the crystal. It scales with volume, and, hence, scales with time: relative center-to-face distances remain constant for all time. Hence

$$\frac{\mathrm{v}(n_1)}{l_1} = \frac{\mathrm{v}(n_2)}{l_2} = \cdots = \frac{\mathrm{v}(n_i)}{l_i} \tag{18}$$

This is the key relation that is used in crystal growth research. In experiments, this equation is used to estimate relative face velocities from measurements of center-to-face distances; in modeling, the shape is constructed from relative face velocities.

The analogy between the growth and equilibrium shapes leads to an important property for the growth shape, one that observers of crystal growth have suggested for a long time (Wells, 1953): *the slower the growth rate of a face, the larger its size on the crystal. Growth shapes are dominated by slow growing faces.*

The overall morphology of a crystal is usually characterized by its *aspect ratio*, defined as the ratio of longest to shortest crystal dimension. This can be approximated by the ratio of largest to smallest $\mathrm{v}(n)$ for facets that appear on the crystal. Crystal shape prediction is therefore primarily concerned with models that predict relative rates of growth. The simplest are based on the influence of anisotropic forces within the crystal structure; the more advanced include the influence of surface-fluid interactions.

Bravais-Friedel, Donnay-Harker Method

The earliest attempt to quantitatively relate crystal habit to crystal structure was proposed by Bravais (1866) and validated by the extensive observations of Friedel (1907). They suggested that the morphological importance $M.I.$ of a face (its relative area on the crystal) is proportional to the interplanar spacing d_{hkl} of its corresponding lattice plane. Donnay and Harker (1937) extended this approach to take into account reductions in interplanar spacing due to space group symmetry, and, hence, it is often termed the Donnay-Harker or the BFDH law. It remains the simplest way to predict the likely forms on a crystal, and can be used in conjunction with the Wulff construction to draw the crystal shape.

The theory is derived from two hypotheses made by Bravais during his pioneering work on crystallography. The concepts are fundamental to the study of crystal growth, and are based on his observations of crystal cleavage. Bravais noted that, for a given material, some crystal faces are more easily cleaved than others. He suggested that:

(I) Faces that are easiest to cleave have strong cohesive forces between molecules in the surface layer, that is, *tangential to the plane,* and weak cohesion forces between adjacent layers, that is, *normal to the plane.*

(II) Forces involved in crystal cleavage are essentially the same as those involved in crystal growth—the most dominant faces grow slowly because they have strong tangential, and weak normal forces.

Bravais went on to approximate the tangential and normal forces at crystal faces. He assumed that strong tangential forces were due to a high density of molecules on a surface layer. Since molecules in the solid state are on the nodes of crystal lattices, the density of material can be represented by the density of nodes. This is, in crystallographic terms, the reticular density, S_{hkl}: the number of nodes per unit area on a net plane (a lattice plane that intersects nodes). It is inversely proportional to the reticular area A_{hkl}: the area of a net plane per node it intersects ($A_{hkl} = 1/S_{hkl}$). Therefore, he proposed, tangential forces are inversely proportional to A_{hkl}. Similarly, he approximated the normal forces by assuming that they are inversely proportional to the distance between layers of material. Large spacing would imply weak interactions. The spacing is represented by the distance between net planes d_{hkl}.

The original hypothesis implied that both normal and tangential forces, now approximated by reticular area and interplanar spacing, have an impact on morphology. However, because $A_{hkl} \cdot d_{hkl} = V$, and V is the constant lattice volume per node, A_{hkl} and d_{hkl} are not independent variables. The most important faces on a crystal have small reticular areas, implying large interplanar spacings, and vice versa. Hence

$$M.I._{hkl} \propto \frac{1}{A_{hkl}} \propto d_{hkl} \tag{19}$$

Since d_{hkl} is large when h, k, and l are small integers, low index faces tend to dominate crystal morphology.

Morphological importance was a term employed by the early researchers of crystal shape. It represented both the frequency of occurrence of a face in a crop of crystals, and its relative size (macroscopic area) on a crystal (Donnay and Harker, 1937). Since the relative area of a face on a growing polygon is approximately inversely proportional to its relative linear velocity (Cahn et al., 1991), $M.I.$ can be approximated by the inverse of velocity, and, hence, the relationship

$$R_{hkl} \propto \frac{1}{d_{hkl}} \tag{20}$$

where R_{hkl} is the velocity of a crystal face with the same normal direction as the net plane (hkl). This relationship yields relative velocities between any number of possible faces, and, hence, can be used to construct the growth shape.

The law originally assumed that there was only one net plane in any crystallographic direction. In many instances this is true: there is only one value of n such that (nh, nk, nl) intersects nodes. Generally $n = 1$, and hkl are small, because the net plane is intersecting nodes which are at lattice vertices. For example, in a cubic lattice, (100) is the only net plane with a normal in the [100] direction. Hence, a crystal face growing in that direction is termed the (100) crystal face, and, by the BFDH law, has a velocity inversely proportional to d_{100}.

Donnay and Harker (1937) discovered exceptions to this due to the symmetry of certain space groups. They found that in crystal structures with centering, glide planes, or screw axes, there are directions that have more than one net plane; that is to say, more than one n such that (nh, nk, nl) intersects nodes. The planes are structurally equivalent, intersecting the same types of molecules and having the same surface densities. They only differ because in one of the planes the molecules are translated and/or rotated relative to the other.

For example, in a body-centered cubic lattice, there are two net planes whose normals are [100]: the (100) plane, intersecting the vertex nodes, and the (200) plane, intersecting the centered nodes. They have the same pattern and density of nodes, but the whole pattern (the "net") has been translated. For an actual crystal face growing in the [100] direction, either net plane could be the surface structures—they are equivalent. Since the (200) family of lattice planes includes both structures, it is labeled the (200) face; its velocity is inversely proportional to d_{200}.

These exceptions to the original law of Bravais are a result of what is termed *effective reductions in interplanar spacing.* In certain space groups, in certain directions, the smallest index family of net planes does not represent the actual spacing of net planes. The smallest index plane is said to be "extinct," excluded from morphological consideration. Because of the symmetry operations within each space group, it is possible to express the indices of extinct planes in algebraic relationships. These *extinction conditions* are well known for each space group, and are available in the X-ray diffraction literature (Hahn, 1995). They play an important role in diffraction experiments, because the same reduction in interplanar spacing that causes morphological extinction also leads to the extinction of diffraction patterns.

The BFDH model is implemented by calculating d_{hkl} for a range of net planes which are potential crystal faces. All that is needed is the unit cell and space group information. It is only necessary to calculate d-spacing for small values of hkl, such as all hkl between 1 and 3, since high index faces are unlikely to appear in the final shape. The planes that satisfy

extinction conditions are also excluded. The number of calculations can be further reduced by ignoring symmetrically equivalent planes, planes of a form. The entire process can be done automatically on a computer, and there are programs available such as MORANG (Docherty and Roberts, 1988a). The d-spacings provide a means of ranking the most morphologically important forms, and yield their relative velocities. Applying a Wulff construction to the velocities gives the BFDH estimate of the growth shape.

Hartman-Perdok Approach

Hartman and Perdok (1955) developed an approach for predicting crystal shape based on similar principles to Bravais'. They too suggested that prominent faces must have strong tangential forces and weak normal forces. However, their model uses actual measures of the chemical interactions, not geometric approximations, to predict face growth rates. There are two principal contributions of Hartman and Perdok that are frequently discussed in the literature: *PBC theory*, a method for defining the morphological importance of various crystal faces, and the *attachment energy model*, a method for predicting, quantitatively, the relative growth rates of faces.

PBC theory stems from the proposition that there are different growth mechanisms and surface structures on faces of different orientation. Low index faces, with their high density of surface molecules, should remain macroscopically flat throughout the growth process, and have a distinct dividing plane between the crystal and ambient phase. High index planes, however, with their large distances between molecules, may exhibit hill and valley structures with no distinct dividing plane. The significance of this is that a molecule crystallizing onto a flat face will have a much higher energy barrier to overcome than one attaching into a hill and valley structure (Hartman, 1953). The flat faces should be slower growing, and dominate the crystal morphology.

Hartman and Perdok proposed a rule of thumb for distinguishing between these different interface structures. First, they defined interactions between centers of mass of growth units (molecules or atoms) as bonds, and since a particular bond is repeated throughout the crystal, they termed these *Periodic Bond Chains* (PBCs). If a face is parallel to at least two ''strong'' PBCs, then they proposed that it must be stable and macroscopically flat (F face); if it has only one ''strong'' PBC then it is moderately rough, or stepped (S face); if it has none, then it is completely kinked and rough (K face). They reasoned that F faces are the most morphologically important, followed by S faces, and then K faces. Thus, the theory may be used to rank the morphologically important forms on a crystal.

The use of PBC theory in this way requires an understanding—or more precisely, an exact definition—of ''strong'' bonds. For metallic and ionic solids, which have highly symmetric growth units and crystal packing, the dominant chemical interactions in the crystal are often assumed to be between nearest neighbor growth units. For these materials, Hartman and Perdok proposed explicitly that the first nearest neighbor interactions are the ''strong'' bonds. For organic crystals, however, they did not propose such a strict definition. Organic molecules and crystal structures are more asymmetric, and it is accepted that there are significant bonds between molecules that do not have the absolute closest centers of mass. Hartman and Perdok suggested that there was a coordination sphere about a central molecule that encompassed all the molecules with which it made strong bonds; unfortunately, they did not provide an exact definition of this sphere. Instead, they relied heavily on chemical intuition—qualitative judgments—to define the strong PBCs in organic materials. The need for qualitative judgments limits the use of this approach. As a result, PBC theory is not as widely employed for ranking morphologically important forms as the BFDH model discussed in the previous section.

Nevertheless, Hartman and Perdok's method for calculating the relative growth rates of faces, the *attachment energy model*, is very widely applied. This technique determines relative growth rates from the magnitude of the intermolecular interactions within crystals. For organics, these interactions are the relatively weak, noncovalent cohesive forces between molecules, although it is also quite common for charge transfer interactions—mainly hydrogen bonds—to exist. The total intermolecular energy per mol in a crystal is termed the lattice energy E^{latt}, which is approximately equal to the negative enthalpy of sublimation. (The lattice energy is the internal energy of the crystal, which is a negative number. The sublimation enthalpy is the energy required to sublime the crystal, which is a heat input to the system, and thus is usually reported as a positive number.) Hartman-Perdok theory partitions the lattice energy into two contributions: the interaction within a slice of thickness d_{hkl}, and the interaction between the molecules in the slice and molecules in the rest of the crystal. The energy per mol within a slice E^{sl} is effectively the energy of formation of a slice from the gas phase. The energy per molecule between the slice and the bulk is effectively twice the energy per molecule of attaching the slice to the underlying crystal. The energy between slice and bulk is termed the attachment energy E^{att}. For any face (hkl), the sum of the slice energy and the attachment energy is a constant E^{latt}

$$E^{\text{latt}} = E^{sl}_{hkl} + E^{att}_{hkl} \tag{21}$$

Hartman and Perdok suggested a relationship between attachment energy and the rate at which material attaches to a face. They assumed that bond energy is inversely proportional to the time required to form a bond. The velocity of a face must therefore increase with increasing magnitude of the attachment energy

$$R_{hkl} \propto |E^{\text{att}}_{hkl}| \tag{22}$$

where R_{hkl} is the rate of growth of face (hkl) in the direction of its normal.

The model implies that faces with larger $|E^{\text{att}}_{hkl}|$ grow faster and are less prominent on a crystal. Since energy is in general a function of intermolecular distance, it is consistent with the Law of Bravais: faces with small interplanar distances have large $|E^{\text{att}}_{hkl}|$. Equation 22, like Eq. 20, gives relative rates of growth that can be used in conjunction with a Wulff construction to draw the shape.

Energy Calculation

The attachment energy method requires calculation of the intermolecular forces within crystals. For molecular crystals, these are dominated by repulsive, dispersive attractive, and electrostatic contributions. The repulsive and attractive (that is, van der Waals) energy shared between two particles is a function of the interparticle distance r, and can generally be described by a potential energy expression. Two common forms are (Gilli, 1992)

$$V_{vdW} = \frac{-A}{r^6} + \frac{B}{r^n} \tag{23}$$

$$V_{vdW} = \frac{-A}{r^6} + B\exp(-Cr) \tag{24}$$

where A, B, C, and n are parameters that depend on the type of particles (type of materials) that are interacting.

These expressions are obeyed only when the interaction between particles is averaged over all orientations, that is, when the particles have spherical symmetry. Hence, potentials of this kind cannot be applied directly to most molecules. However, they can be applied to force centers in molecules, namely atoms. The sum of all atom-atom interactions between two molecules approximates the total molecule-molecule interaction. This *atom-atom approximation* has been shown to be valid for a great variety of molecular systems (Kitaigorodsky, 1973).

Electrostatic contributions to the energy of organic crystals are mostly due to dipole-dipole and hydrogen bonding interactions. Because of the difficulty in ascribing localized dipole moments, the monopolar model of the electrostatic forces is often used (see Kitaigorodsky, 1973). Partial charges are assigned to all atoms, and the coulombic energy shared between two atoms is given by

$$V_{\text{elec}}(r) = \frac{q_1 q_2}{Dr} \tag{25}$$

In addition, this monopolar model is also a physically reasonable interpretation of the hydrogen bond (Hagler et al., 1974). Thus, hydrogen bond energy can be calculated using Eq. 25. The accuracy of this technique depends on the choice of partial charges, which are parameters that depend on atom type just like the parameters in the van der Waals terms. The complete expression for the atom-atom potential is therefore

$$V = V_{vdW} + V_{\text{elec}} \tag{26}$$

Sometimes an additional term V_{hb} is employed to account for the dependence of hydrogen bonding on the geometry of donor-hydrogen-acceptor atoms.

Several forms of Eq. 26 have been parameterized for organic materials. They include the force fields of Kitaigorodsky et al. (1968), Williams (1966), Momany et al. (1974), and Lifson, Hagler and Dauber (1979), each of which are accurate for a specific class or classes of compounds (such as alkanes, carboxylic acids, and so on). The more generic DREIDING force field (Mayo et al., 1990), although not as precise as the older models, has parameters for a large number of main group elements and is suitable for a wide range of organic materials. Some of the force fields include partial charges for atom types in a class of compounds; these have been selected so as to predict the known electrostatic and hydrogen bonding characteristics of these materials. When partial charges are not provided, it is reasonable to use gas-phase charges in the coulombic term that are calculated by *ab intio* or semi-empirical quantum mechanics methods.

Potential functions in the form of Eq. 26 are employed to calculate E^{latt}. The lattice energy is half the sum of all atom-atom interactions between a central molecule and the surrounding molecules in the crystal. If the central molecule and the N surrounding molecules each have n atoms, then

$$E^{\text{latt}} = \frac{1}{2}\sum_{k=1}^{N}\sum_{i=1}^{n}\sum_{j=1}^{n} V_{kij} \tag{27}$$

where V_{kij} is the interaction of atom i of the central molecule with atom j of the kth surrounding molecule. The accuracy of Eq. 27, and, hence, the accuracy of the chosen potential set, is tested by comparison to the experimental sublimation enthalpy of the material of interest. The lattice energy must satisfy the relationship

$$B^{\text{latt}} = -\Delta H^{\text{sub}} - 2RT \tag{28}$$

where the $2RT$ compensates for thermal contributions to the enthalpy (Gilli, 1992).

The number of summations in Eq. 27 is, in principle, infinite. However, in practice, it is finite, because only molecules within a fixed distance from the central molecule contribute significantly to the energy. The cutoff radius can be determined by repeatedly calculating E^{latt} with greater and greater numbers of surrounding molecules until there is negligible decrease in the energy. For many organics, this occurs at a distance of about 15 to 20 Å from the central molecule. During the lattice energy calculation, slice and attachment energies can also be determined. For a face (hkl), boundaries of the slice are constructed around a central molecule. Interactions with molecules whose center of mass is within the boundaries contribute to the slice energy. Those outside of the boundary contribute to attachment energy. This is illustrated in Figure 2. If there is more than one choice for the central molecule, that is, more than one independent molecule in the unit cell, the slice is centered at each one, and the energy results are averaged. This general procedure —setting up the lattice, applying an intermolecular potential, determining the cut-off radius, and calculating E^{latt}, E^{sl}, E^{att} —has been implemented by several authors (Saska and Myerson, 1983; Berkovitch-Yellin, 1985; Docherty and Roberts, 1988b), and there are two publicly available programs for this purpose: HABIT (Clydesdale et al., 1991) and Cerius.

Crystal Shape Predictions

Adipic acid

Adipic acid is a precursor to Nylon and is a widely produced industrial chemical. It is also used as a lubricant and acidulant in pharmaceutical tablet formulations. Its crystal

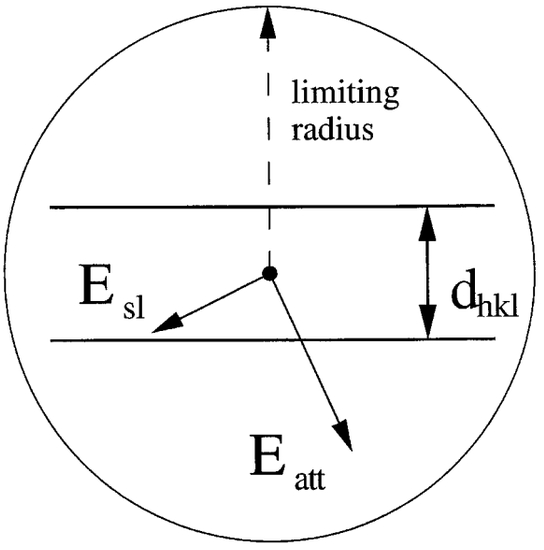

Figure 2. Attachment energy calculation.

shape plays a major role in the material's bulk processing; in particular, certain shapes are dominated by hydrophilic faces that make flowability very difficult (Klug and van Mil, 1994). Adipic acid shape also has a large effect on tablet compaction and dissolution properties, and, hence, is of great interest to pharmaceutical researchers (Chan and Grant, 1989; Grant et al., 1991). The effect of impurities, additives, and solvents on adipic acid crystal shape is an active area of study (Myerson and Saska, 1990; Pfefer and Boistelle, 1996).

The BFDH and attachment energy models were used by Davey et al. (1992) to predict adipic acid crystal shape, and a similar calculation has been repeated here. Table 1 lists interplanar spacings and attachment energies of various low index faces, in units of Angstroms and kcal/mol, respectively. Adipic acid crystallizes in space group $P2_1/c$, with two molecules per unit cell, and unit cell dimensions: $a = 10.01$, $b = 5.15$, $c = 10.06$, and $\beta = 136.75°$ (Housty and Hospital, 1965). Its extinction conditions are: $h0l$ $l = 2n$, $0k0$ $k = 2n$, hkl $k + l = 2n$. The energy calculation was performed with a 6-12 potential developed by Lifson et al. (1979) for carboxylic acids and amines. The potential also included estimates of partial charges that are suitable for carboxylic acids. The calculated lattice energy was -35.5 kcal/mol, which compares well to the enthalpy of sublimation, 32.1 kcal/mol (Lifson et al., 1979).

Table 1. BFDH and Attachment Energy Results for Adipic Acid

Face	d_{hkl} (Å)	E^{att}_{hkl} (kcal/mol)
100	6.920	−25.68
$10\bar{2}$	4.767	−26.98
$20\bar{2}$	4.685	−31.27
$11\bar{1}$	4.513	−27.32
$01\bar{1}$	4.126	−12.95
$2\bar{1}\,\bar{1}$	3.509	−31.42
002	3.446	−15.29

It is important to note the disagreement between the BFDH and attachment energy results (see Figure 3). The (100) face has a large slice thickness, yet it has a large attachment energy. This is a result of a chain of strong hydrogen bonds along the [100] direction, which contribute significantly to the attachment energy. The BFDH crystal is dominated by a slow growing (100) face, while the attachment energy crystal is fast growing and elongated in this direction.

Also shown is the flat, plate-like, adipic acid crystal grown from aqueous solution (redrawn from Davey et al., 1992). Studies have shown that polar solvents like water and cationic additives reduce the (100) growth rate resulting in plate-like, even flaky shapes (Michaels and Colville, 1960). Nonpolar solvents, anionic additives, and growth from the vapor permit fast (100) growth and, hence, result in needle-like crystals (Klug and van Mil, 1994).

Several attempts to model the effects of solution phase on adipic acid crystal shape have been reported in the literature. Myerson and Saska (1990) have calculated the solvent accessible regions of adipic acid faces, an approach generally applied to biochemical structures. Davey et al. (1992) have ex-

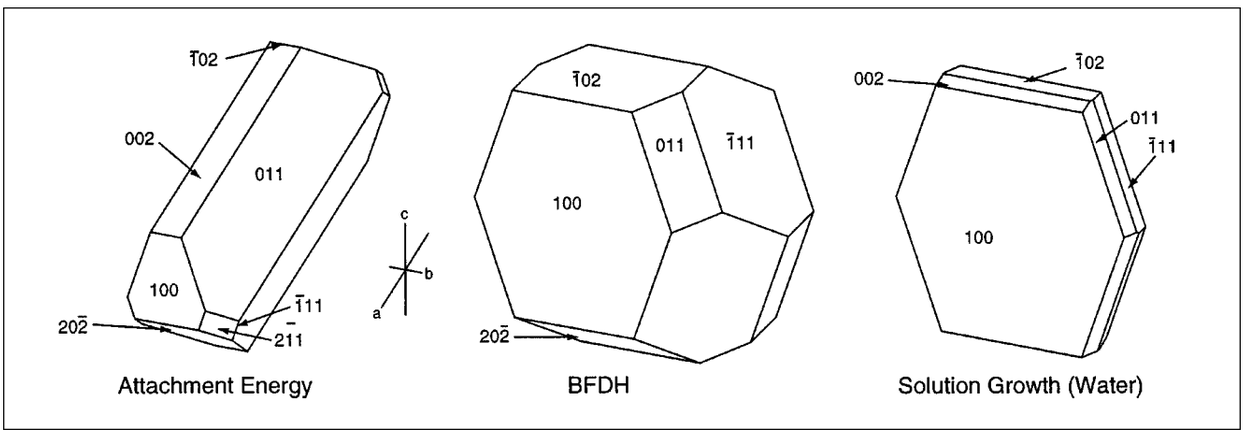

Figure 3. Adipic acid crsytals.

Water grown crystal redrawn from Davey et al. (1992).

amined structurally similar impurities in a tailor-made additive type approach. These strategies have not been completely successful, and are not effective for routine, *a priori* predictions of crystal shape.

Ibuprofen

Expanding world markets and increased competition have ignited efforts to improve pharmaceutical production. Ibuprofen is an example of a widely used medication whose process efficiency and product quality were improved by modifying the crystallization process. By changing the solvent from linear alkanes to linear alcohol/alcohol mixtures with high hydrogen bonding solubility parameters δh, more equant crystal shapes were achieved (see U.S. Patent 4,476,248, Gordon and Amin, 1984). These shapes caused less lamination of tablet compression dies and, hence, less production downtime. Tablet integrity, shelf life, and the drug's bioavailability were also enhanced.

A method for selecting the proper solvent *a priori* would be a valuable tool for process design. The BFDH and attachment energy models were explored as a first approach. Such a simulation has been performed by Bunyan et al. (1991), where the growth unit was assumed to be the individual ibuprofen molecules. However, ibuprofen molecules pack in the lattice as dimers, and it is possible that the dimer is the growth unit that enters the solid phase. There is some evidence that mono-carboxylic acids like ibuprofen form dimer precursors in the solution (Gavezzotti et al., 1997). In this study, the morphological models were applied to both the monomer and the dimer case for comparison.

Racemic ibuprofen is in space group $P2_1/c$, with $a = 14.667$, $b = 7.866$, $c = 10.730$, $\beta = 99.36°$, and four molecules (two dimers) per unit cell (McConnell, 1974). The general extinction conditions are $h0l\ \ l = 2n$, $0k0\ \ k = 2n$. The dimer has a symmetry center situated on a "special" position in this space group while the monomer does not; thus, the special extinction condition $hkl\ k + l = 2n$ is only applied in the dimer case.

Since ibuprofen is an aromatic with a carboxylic acid side chain, the potential of Lifson et al. (1979) was used for the energy calculation. This force field includes parameters and partial charges for the carboxylic and alkyl portions of the molecule, but none for atoms in the aromatic portion. As an approximation, the alkyl parameters are applied to these atoms, although this might be expected to reduce the accuracy of the energy calculation. Nevertheless, the predicted lattice energy for the monomer simulation was 29.3 kcal/mol, which compares well to the experimental sublimation enthalpy of 28.9 reported by Bunyan et al. (1991).

Table 2 gives the results of the BFDH and attachment energy calculations, and Figure 4 illustrates the predicted shapes. These can be compared to the experimental shapes reported by Bunyan et al. (1991) for ibuprofen crystals grown from hexane, ethanol, methanol, and from the vapor (Figure 5). Note that the (110) and $(2\bar{1}0)$ faces are excluded from the dimer calculation because of the special condition. Both of the predicted crystals are similar to the sublimation crystal—flat plates dominated by the (100) face. However, the dimer calculation appears to be the better prediction, since it yields {011} as the dominant form for growth in the direction of the b-axis. Neither prediction matches the solvent-grown shapes: the hexane (low δ_h) shape is needle-like with an aspect ratio of about 8, while the ethanol and methanol (high δ_h) shapes have aspect ratios close to 2. The latter is known to be the preferred shape for downstream processing and end-product quality (Gordon and Amin, 1984).

Table 2. BFDH and Attachment Energy Results for Racemic Ibuprofen

Face	d_{hkl} (Å)	E^{att}_{hkl} (kcal/mol)	E^{att}_{hkl} (kcal/mol·dimer)
100	14.47	−12.03	−9.59
110	6.92	−17.53	
011	6.32	−19.32	−35.20
$11\bar{1}$	6.01	−20.08	−35.61
$1\bar{1}1$	5.60	−23.58	−34.23
$2\bar{1}0$	5.33	−21.56	
002	5.29	−26.28	−31.45
$10\bar{2}$	5.25	−25.02	−35.35

Because the models do not predict the solvent-grown shape, a qualitative interpretation of the solvent effect is sometimes proposed. In an analysis akin to the *tailor-made additive* approach, Bunyan et al. (1991) suggested that polar solvents are likely to inhibit the growth of faces which have accessible sites for hydrogen bonding. However, this explanation is not valid if the dimer is the growth unit, where no carboxyl groups are available to the solvent. For the hexane-grown needle shape, Bunyan and co-workers suggested that dimers made up of R-R and S-S enantiomers may act as impurities to inhibit the growth of certain faces.

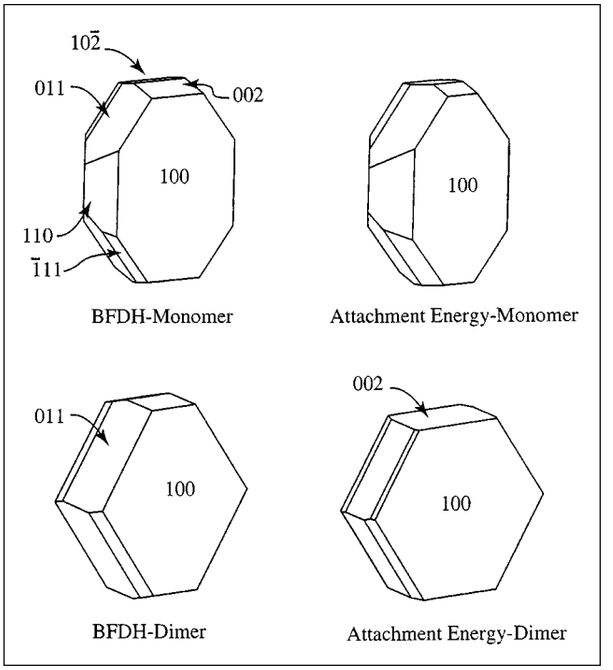

Figure 4. Predicted crystal shapes of racemic ibuprofen.

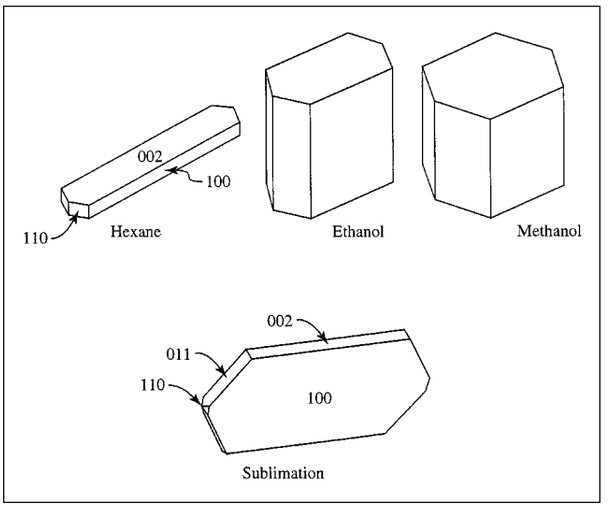

Figure 5. Experimental shapes of ibuprofen crystals.
Redrawn from Bunyan et al. (1991).

Detailed Kinetics: Solvent Effect

Both the BFDH and attachment energy models are based on sound physical principles; however, they have two main drawbacks: (1) The theories are based on the physics of the internal crystal structure, and ignore effects from the external environment; (2) the theories do not provide a precise mechanism for solute incorporation, and, hence, it is unclear how one might include external factors, like solvent effects, in the models. In order to have a better understanding of the growth process and a more accurate prediction of crystal shape, especially when grown from solution, it appears necessary to use a detailed kinetic model of crystal growth.

The recent work of Liu et al. (1995) has shown promise as a means of modeling the effects of crystallization environment on the shapes of organic crystals. They have successfully predicted the effects of solvent on the shape of several organic crystal systems. The method is derived from well known kinetic theories of crystal growth: the BCF model (Burton et al., 1951) and its variations [such as the Chernov model (Chernov, 1984)], and 2-D nucleation growth models. For each mechanism, relative growth rate expressions have been formulated. Applying the approach to a given crystal system requires an initial assumption about the type of crystal growth mechanism that occurs.

We will briefly discuss the method of Liu and Bennema, using their interpretation of the Chernov model as an example. The focus will be on the important habit controlling face-depending factors (anisotropic variables), and we refer the reader to the Appendix for a full derivation. The Chernov model is based on the BCF theory, which proposes that facetted crystals grow due to the lateral movement of microscopic steps across faces, and that these steps are the edges of spirals arising from dislocations on crystal faces (Figure 6). Chernov suggested that, in solution growth, the rate limiting step for the movement of edges is the incorporation of material into kink sites in the edges. The growing, moving edges cause the spiral to rotate, facilitating continuous normal growth of the macroscopic face.

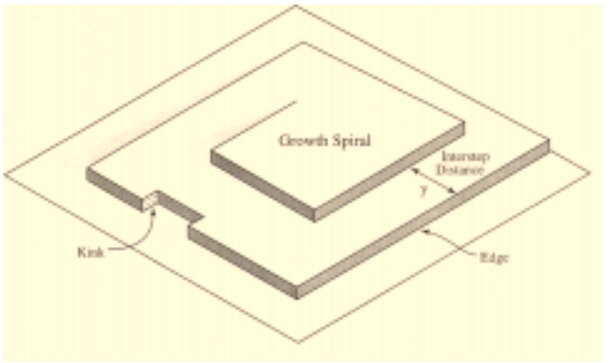

Figure 6. Spiral growth on a macroscopically flat face.

Based on principles of step geometry and step flow, BCF formulated an expression for the rate of growth normal to a surface with laterally propagating steps

$$R = \upsilon \times h/y \tag{29}$$

where υ is the lateral velocity of steps, y is the distance between steps, and h is the step height, normally thought to be d_{hkl}. The parameters y and υ depend on the number of steps on a face, the number of kinks on a step, the step (spiral) geometry, and the rate at which material is added to kink sites. The Chernov model assumes that kink integration is the rate limiting step, and, thus, the primary anisotropic variable affecting step velocity is the probability of finding a kink on an edge

$$\upsilon \propto \frac{a}{\lambda_0}\left(1+\frac{1}{2}\exp\left(\phi^{\text{kink}}/kT\right)\right)^{-1} \tag{30}$$

where ϕ^{kink} is the energy to form a kink, a is the molecular distance, and λ_0 is the distance between kinks. The main face dependent factor affecting y is the energy to form an edge, which itself depends on ϕ^{kink} (Liu et al., 1995). The kink energy is therefore the key anisotropic physical property that dominates the morphological prediction.

As seen in Figure 6, the kink energy is the work required to form an edge of molecular size orthogonal to a macroscopic edge. If the crystal is growing in a vacuum, then this is just the work required to break the bond between the molecules along the edge—the breaking of a bond along one of Hartman and Perdok's PBCs. However, with a solvent present, the work must include the change in energy associated with having a solvent in contact with the kink. This may include both a change in internal energy due to the breaking and making of bonds, but also entropic contributions due to the different state of the solvent. Thus, the kink energy might more correctly be termed the kink free energy. In Liu and Bennema's development, however, only the change in forces (internal energy) are considered, and, thus, it is termed kink energy.

The formation of a kink between crystal and solvent is similar to the dissolution of a solid in a solvent: the solid–solid

bonds and solvent–solvent bonds are broken, and solid–solvent bonds are formed. Thus, the energy to form a kink might be approximated by some fraction of the enthalpy of dissolution. Using the proportionality approximation, one can assume that there is a fraction of ΔH^{diss} that is due to changes in interactions in the lateral direction—parallel to the slice—and that this can be divided by the number of nearest neighbors in the slice to yield the individual kink energies on the face

$$\phi_{hkl}^{\text{kink}} = \xi_{hkl} \Delta H_{hkl}^{\text{diss}} / n_{hkl} \tag{31}$$

where $\xi_{hkl} = E_{hkl}^{sl} / E^{\text{latt}}$ and is the anistropy factor that determines the proportion of bonds in the lateral direction (in the slice), and n_{hkl} is the number of nearest neighbors parallel to the face. This expression can be further refined by assuming that there is a local solution phase with its own $\delta H_{hkl}^{\text{diss}}$ in contact with each face on the crystal. Using the regular solution model for the dissolution enthalpy, we can write

$$\ln X_A^0 \propto \Delta H^{\text{diss}} \tag{32}$$

$$\ln X_{A(hkl)}^{0(\text{eff})} \propto \Delta H_{hkl}^{\text{diss}} \tag{33}$$

and define the factor C_{hkl}

$$C_{hkl} = \frac{\Delta H_{hkl}^{\text{diss}}}{\Delta H^{\text{diss}}} = \frac{\ln X_{A(hkl)}^{0(\text{eff})}}{\ln X_A^0} \tag{34}$$

where X_A^0 is the bulk concentration of solute (A) in solution and $X_{A(hkl)}^{0(\text{eff})}$ is the local concentration of solute in proximity to a given crystal face. Since all other factors in the model can be determined from attachment energy calculations and structure considerations, C_{hkl} is the only measure of the solvent effect, and the key input to crystal shape prediction. In fact, C_{hkl} is the key habit controlling factor in all the mechanism explored by Liu and Bennema (1996a). In order to apply this method, $X_{A(hkl)}^{0(\text{eff})}$ and C_{hkl} are determined *a priori* by molecular dynamcis modeling (Boek et al., 1994) or self-consistent field calculations (Liu and Bennema, 1993a) of the solid–solution interface.

We have recently developed a similar approach for predicting crystal shape based on the same detailed kinetic principles (Winn and Doherty, 1998, 1999). The kink energy is again the key habit determining factor, but it is calculated with the use of surface properties of the crystal and solvent. The kink, though it is a surface of molecular dimensions, is assumed to be a macroscopic surface with a specific surface free energy. This property is dominated by internal energy—the breaking of bonds—whose magnitude can be determined from attachment energy simulations. The solvent property is its surface free energy, which is generally known for many substances (Kaelble, 1971). The two properties can be combined in a classical approach (Girifalco and Good, 1957) to yield the interfacial free energy at the kink

$$\gamma^{\text{kink}} = \gamma^{\text{cryst}} + \gamma^{\text{solv}} - 2\sqrt{\gamma^{\text{cryst}} \gamma^{\text{solv}}} \tag{35}$$

where γ^{cryst} is the surface free energy of the crystal at the kink site and γ^{solv} is the surface free energy of the solvent. The kink interfacial free energy γ^{kink} has units of energy per kink area, which can be converted to units of energy per kink to yield the work to form the kink. This method has be used to predict the effects of solvent on the shape of adipic acid and ibuprofen crystals (Winn and Doherty, 1998, 1999).

The two techniques discussed above are similar in that they are based on detailed kinetic theories, where the kink energy is the main habit controlling factor. Also, both methods require information obtained from attachment energy simulations. In the method of Liu and Bennema, the solvent effect is determined by the molecular level simulation of the solvent–crystal interface. Thus, it may be less efficient for process engineering applications than the method of Winn and Doherty, where the solvent effect is determined from known properties of the pure solvent. Both methods, however, are new, and their efficacy and value for morphology prediction need to be further explored.

Crystal Shape Predictions: Solvent Effects

Adipic acid grown from water

Adipic acid, which is a dicarboxylic acid, has a crystal structure dominated by hydrogen bonding. The molecules form chains of hydrogen bonds, which are packed together with dispersive forces. The interaction of a polar solvent, such as water, at kink sites on the crystal surface dramatically affects the shape. Winn and Doherty (1998) have identified the three principal PBCs on the surface structure of adipic acid; two are dispersive and the third is hydrogen bonded. The kink interfacial free energies between crystal and water were calculated at the dispersive sites using Eq. 35 (Winn and Doherty, 1998), and at the hydrogen bond site using the Karger et al. (1976) proton donor-acceptor model (Winn and Doherty, 1999). The calculated kink free energies were used in a screw dislocation model for face growth to produce relative face growth rates. The predicted crystal shapes are shown in Figure 7 and are close to the experimental shape shown in Figure 8.

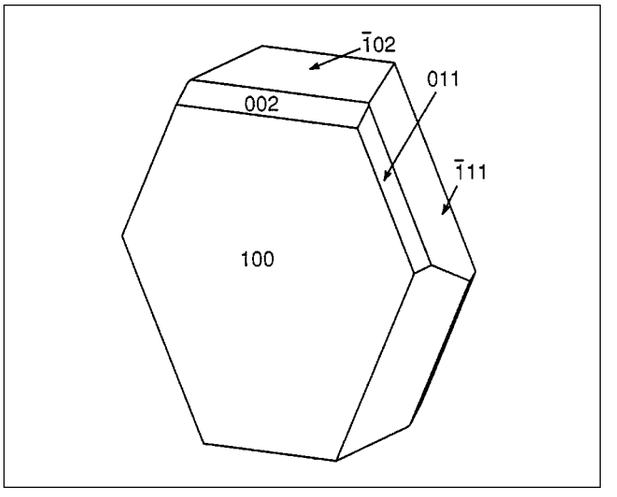

Figure 7. Predicted morphology of adipic acid grown from water.

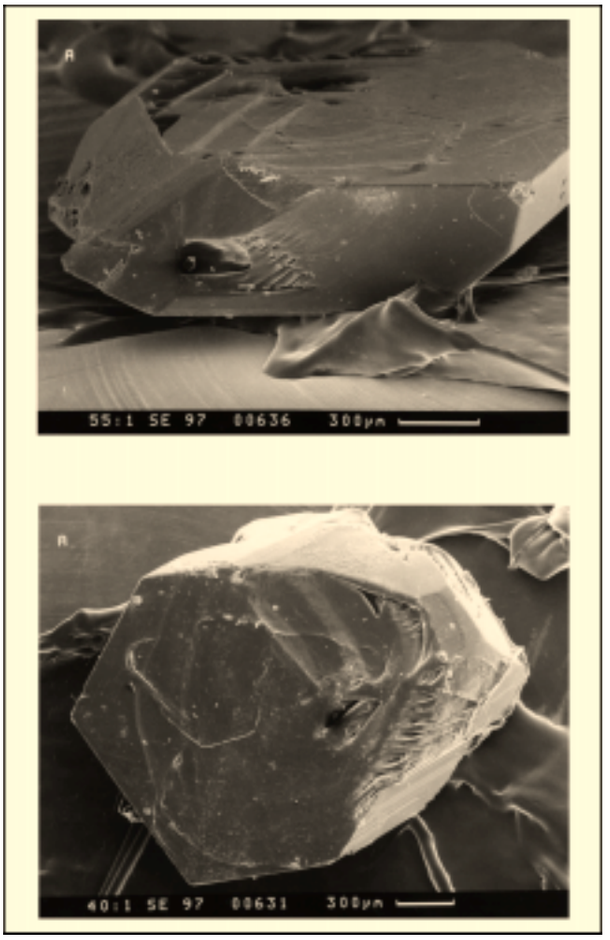

Figure 8. Two views of an adipic acid crystal grown from aqueous solution.

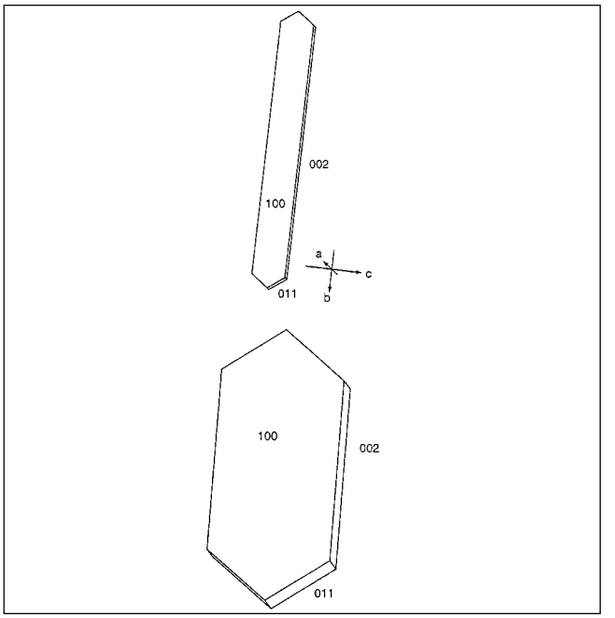

Figure 9. Predicted morphology of ibuprofen crystals grown from hexane (top) and methanol (bottom).

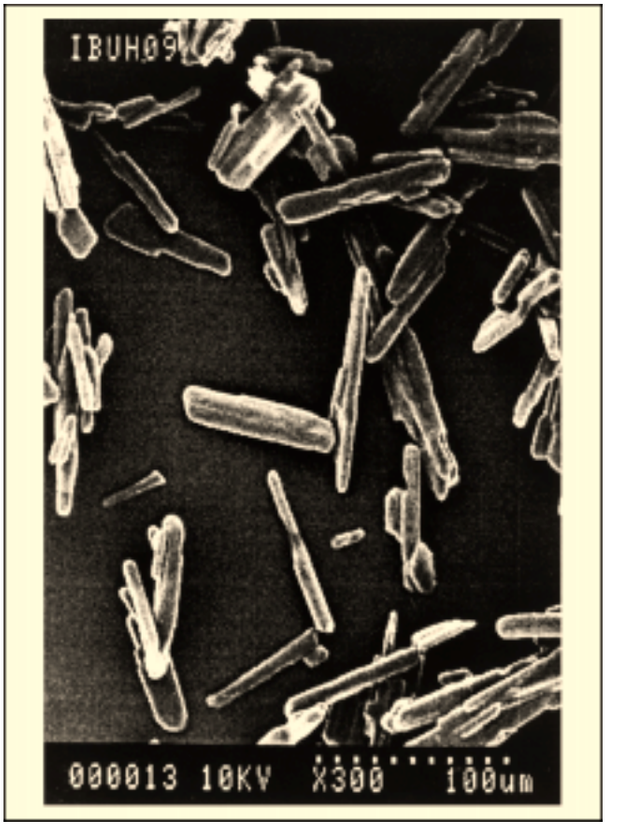

Figure 10. Ibuprofen crystals grown from hexane.
Courtesy of Storey (1997).

Ibuprofen grown from hexane and from methanol

The crystal structure of ibuprofen is an arrangement of hydrogen-bonded dimers interacting with dispersive forces. Like most monocarboxylic acids, it is thought that this packing stems from dimer formation in solution prior to incorporation into the crystal (Gavezzotti et al., 1997). The growth unit is the nonpolar entity of the ibuprofen dimer. All PBCs in the structure (Winn and Doherty, 1998) are formed by dispersive forces–the crystal surface structures do not form hydrogen–bonded interfaces with the solvent.

Because of these characteristics, it is expected that the crystal will form high free energy interfaces with polar solvents, and low free energy interfaces with nonpolar solvents. When Eq. 35 was applied to ibuprofen grown from hexane, the resulting kink free energies were low enough to suggest a 2-D nucleation mechanism of growth (Winn and Doherty, 1998). Conversely, when the solvent is methanol, the higher kink free energies suggest the screw dislocation mechanism. Relative face growth rates have been estimated in both cases, and the shapes are drawn in Figure 9. These shapes are very similar to crystals grown experimentally by Storey and York (Storey, 1997). See Figures 10 and 11.

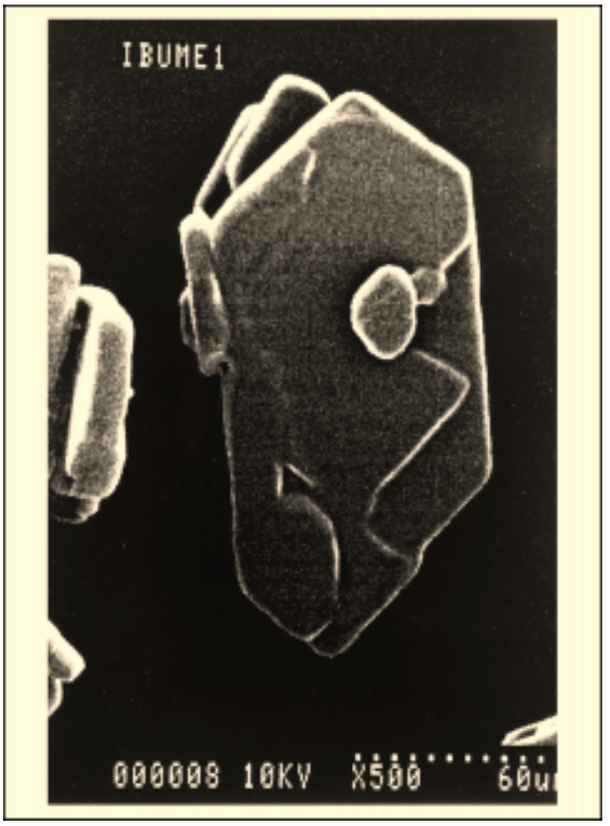

Figure 11. Ibuprofen crystal grown from methanol.
Courtesy of Storey (1997).

Other systems

Detailed growth models have successfully predicted the shapes of other organic crystals grown from solution, including: urea grown from water (Liu and Bennema, 1996c), succinic acid grown from water and from isopropanol (Winn and Doherty, 1999), biphenyl grown from toluene (Liu and Bennema, 1996c; Winn and Doherty, 1998), and naphthalene grown from toluene (Liu and Bennema, 1996c). The general approach seems a promising direction for future research.

Conclusions and Future Directions

The Wulff construction is the key idea that enables the calculation of crystal shape. It can be applied to both the equilibrium and growth forms, using either surface free energies, or relative growth rates, respectively. Despite the complementary nature of face velocity and surface free energy, it is necessary to have a clear distinction between the two. As methods develop for modeling the influence of the solution environment on crystal shape, it is important to distinguish between effects on surface free energy (the equilibrium shape), and effects on growth velocities (the growth shape).

The BFDH and attachment energy models are first-order approaches for predicting morphology, and are very effective at estimating the likely faces on a crystal. Their computer implementations are fast and easy to use, and they have proven to be accurate for predicting vapor-grown crystal shapes. These methods also yield geometric and energetic data that may be useful as input to more detailed kinetic models. The main drawback of these approaches is their inability to account for effects of solvent and other process conditions (that is, impurities and supersaturation).

The approaches of Liu and Bennema, and Winn and Doherty are the first attempts at using detailed kinetic theory for crystal shape prediction. The input to the Liu and Bennema model is obtained from molecular simulation of the solution phase, which may be a drawback for process engineering applications. Both models recognize the significance of interfacial phenomena in crystal shape modeling, and lead the way for future developments, such as new simulation and/or group contribution methods for interfacial free energy prediction.

Some of the key areas for future experimental and modeling research are:

(1) *Mixed Solvents:* Crystals grown from a mixture of two or more solvents can have different characteristics than those grown from any one of the solvents alone. This effect is especially significant if the solute has a very different solubility in each solvent. We are not aware of any modeling studies for mixed solvents, although it is a natural extension of the work described in this article.

(2) *Growth Unit:* The ibuprofen example illustrates that consideration of the growth unit is an important factor in morphology. Several researchers have discussed pre-condensation in the solution phase, and the need to account for this effect in morphological modeling (Geert-man and van der Heijden, 1992; Grimbergen and Bennema, 1996).

(3) *Polymorphs:* Polymorphs have always been of interest in crystallization, but have become a critically important factor in pharmaceutical production and registration because of recent FDA requirements. Different polymorphs have different crystal structures, optical properties, dissolution rates, shapes, and interfacial properties. Thus, models of solution–crystal interactions might be able to predict polymorph selection and/or transition. Systematic studies along these lines would be of great practical interest.

(4) *Chiral Separations:* Single-enantiomer product molecules are a rapidly growing sector of the pharmaceutical industry, and crystallization is one of the key technologies for chiral selection. Crystals of the racemate have different structures than the individual enantiomers. As with polymorphism, interfacial phenomena may influence enantiomeric selectivity, and the challenge is to develop technology, and protocols (aided by modeling) to produce single enantiomer products.

(5) *Process Modeling:* An important and challenging area for chemical engineering research is to link interfacial models, capable of capturing the above effects, to process models. Such models would allow for novel designs and operating protocols to be developed systematically before they are tested experimentally. This is one of the ways that engineering can contribute to faster process development.

Acknowledgments

This research was supported by the University of Massachusetts Process Design and Control Center. Special thanks to Professor Peter York, University of Bradford, U.K., who provided the photograhs of solution-grown ibuprofen crystals.

Literature Cited

Bennema, P., and G. H. Gilmer, "Kinetics of Crystal Growth," *Crystal Growth: An Introduction*, P. Harman, ed., North-Holland, Amsterdam (1973).

Bennema, P., "On the Crystallographic and Statistical Mechanical Foundations of the Forty-Year Old Hartman-Perdok Theory," *J. Crystal Growth*, **166**, 17 (1996).

Boek, E. S., W. J. Briels, and D. Feil, "Interfaces between a Saturated Aqueous Urea Solution and Crystalline Urea: A Molecular Dynamics Study," *J. Phys. Chem.*, **98**, 1674 (1994).

Berkovitch-Yellin, Z., "Toward an ab Initio Derivation of Crystal Morphology," *J. Am. Chem. Soc.*, **107**, 8239 (1985).

Berkovitch-Yellin, Z., J. van Mil, L. Addadi, M. Idelson, M. Lahav and L. Leiserowitz, "Crystal Morphology Engineering by Tailor-Made Inhibitors: A New Probe to Fine Intermolecular Interactions," *J. Am. Chem. Soc.*, **107**, 3111 (1985).

Bermingham, S. K., A. M. Neumann, H. J. M. Kramer, P. J. T. Verheijen, G. M. van Rosmalen, and J. Grievink, "A Design Procedure and Predictive Models for Solution Crystallization Processes," *Fifth Int. Conf. on Foundations of Computer-Aided Process Design*, Breckenridge, CO. M. F. Malone and J. A. Trainham, eds., AIChE, New York (2000).

Bravais, A., *Études Crystallographiques*, Gauthier-Villars, Paris (1866).

Bunyan, J. M. E., N. Shankland, and D. B. Sheen, "Solvent Effects on the Morphology of Ibuprofen," *Particle Design Via Crystallization*, Ramanarayanan, R. W. Kern, M. Larson, and S. Sikdar, eds., AIChE, New York (1991).

Burton, W. K., N. Cabrera, and F. C. Frank, "The Growth of Crystals and the Equilibrium Structure of their Surfaces," *Phil. Trans. Roy Soc.*, **A243**, 299 (1951).

Cabrera, N., and M. Levine, "On the Dislocation Theory of Evaporation of Crystals," *Phil. Mag.*, **1**, 450 (1956).

Cahn, J. W., J. E. Taylor, and C. A. Handwerker, "Evolving Crystal Forms: Frank's Characteristics Revisited," *Sir Charles Frank, OBE, FRS, An Eightieth Birthday Tribute*, R. G. Chambers, J. E. Enderby, and A. Keller, eds., Hilger, New York (1991).

Chan, H., and D. J. W. Grant, "Influence of Compaction on the Intrinsic Dissolution Rate of Modified Acetaminophen and Adipic Acid Crystals," *Int. J. Pharm.*, **57**, 117 (1989).

Chernov, A. A., "The Kinetics of the Growth Forms of Crystals," *Sov. Phys. Cryst.*, **7**, 728 (1963).

Chernov, A. A., *Modern Crystallography III*, Springer-Verlag, New York (1984).

Clydesdale, G., R. Docherty, and K. J. Roberts, "HABIT—A Program for Predicting the Morphology of Molecular Crystals," *Comp. Phys. Comm.*, **64**, 311 (1991).

Clydesdale, G., K. J. Roberts and R. Docherty, "Modeling the Morphology of Molecular Crystals in the Presence of Disruptive Tailor-Made Additives," *J. Crystal Growth*, **135**, 331 (1994).

Curry, J. E., and J. H. Cushman, "Nanophase Coexitence and Sieving in Binary Mixures Confined Between Corrugated Walls," *J. Chem. Phys.*, **103**, 2132 (1995).

Davey, R., W. Fila, and J. Garside, "The Influence of Biuret on the Growth Kinetics of Urea Crystal from Aqueous Solutions," *J. Crystal Growth*, **79**, 607 (1986).

Davey, R. J., S. N. Black, D. Logan, S. J. Maginn, J. E. Fairbrother and D. J. W. Grant, "Structural and Kinetic Features of Crystal Growth Inhibition: Adipic Acid Growing in the Presence of n-Alkanoic Acids," *J. Chem. Soc. Faraday Trans.*, **88**, 3461 (1992).

Davey, R. J., "Looking Into Crystal Chemistry," *The Chemical Engineer*, (Dec. 1991).

Docherty, R., and K. J. Roberts, "Morang—A Computer Program Designed to Aid in the Determination of Crystal Morphology," *Comp. Phys. Comm.*, **51**, 423 (1988a).

Docherty, R., and K. J. Roberts, "Modelling the Morphology of Molecular Crystals; Application to Anthracene, Biphenyl and β-Succinic Acid," *J. Crystal Growth*, **88**, 159 (1988b).

Docherty, R., K. J. Roberts, V. Saunders, S. Black, and R. J. Davey, "Theoretical Analysis of the Polar Morphology and Absolute Polarity of Crystalline Urea," *Faraday Discuss.*, **95**, 11 (1993).

Donnay, J. D. H., and D. Harker, "A New Law of Crystal Morphology Extending the Law of Bravais," *Amer. Min.*, **22**, 446 (1937).

Frank, F. C., "On the Kinematic Theory of Crystal Growth and Dissolution Processes," *Growth and Perfection of Crystals*, R. H. Doremus, B. W. Roberts, and D. Turnbull, eds., Wiley, New York (1958).

Frank, F. C., "On the Kinematic Theory of Crystal Growth and Dissolution Processes, II," *Z. Phys. Chem.*, **77**, 84 (1972).

Friedel, M. G., "Études Sur la loi de Bravais," *Bull. Soc. Franc. Miner.*, **9**, 326 (1907).

Gavezzotti, A., G. Filippini, J. Kroon, B. P. van Eijck, and P. Klewinghaus, "The Crystal Polymorphism of Tetrolic Acid: A Molecular Dynamics Study of Precursors in Solution, and Crystal Structure Generation," *Chem. Eur. J.*, **3**, 893 (1997).

Geertman, R. M., and A. E. D. M. van der Heijden, "On the Morphology of Caprolactam," *J. Crystal Growth*, **125**, 363 (1992).

Gibbs, J. W., *The Collected Works of J. Willard Gibbs*, Yale University Press, New Haven (1928).

Gilli, G., "Molecules and Molecular Crystals," *Fundamentals of Crystallography*, C. Giacovazzo, ed., Oxford University Press, Oxford (1992).

Gilmer, G. H., and P. Bennema, "Simulation of Crystal Growth with Surface Diffusion," *J. Appl. Phys.*, **43**, 1347 (1972).

Girifalco, L. A., and R. J. Good, "A Theory for the Estimation of Surface and Interfacial Energies: I. Derivation and Application to Interfacial Tension," *J. Phys. Chem.*, **61**, 904 (1957).

Glasstone, S., K. J. Laidler, and H. Eyring, *The Theory of Rate Processes*, McGraw-Hill, New York (1941).

Gordon, R. E., and S. I. Amin, "Crystallization of Ibuprofen," U.S. Patent Number 4,476,248 (1984).

Grant, D. J. W., K. Y. Chow, and H. Chan, "Modification of the Physical Properties of Adipic Acid by Crystallization in the Presence of n-Alkanoic Acids," *Particle Design Via Crystallization*, Ramanarayanan, R. W. Kern, M. Larson, and S. Sikdar, eds., AICHE, New York (1991).

Grimbergen, R. F. P., and P. Bennema, "An Automated Method for PBC Analyses Applied to Benzoic Acid: A Comparison Between the Monomer and Dimer Analysis," *Crystal Growth of Organic Materials*, A. S. Myerson, D. A. Green, and P. Meenan, eds., ACS, Washington (1996).

Hagler, A. T., E. Huler, and S. Lifson, "Energy Functions for Peptides and Proteins. I.," *J. Am. Chem. Soc.*, **96**, 5319 (1974).

Hahn, T., *International Tables for Crystallography*, 4th ed., Dordrecht, Boston (1995).

Hartman, P., "Relations between Structure and Morphology of Crystals," PhD Diss., University of Groningen, The Netherlands (1953).

Hartman, P., and W. G. Perdok, "On the Relations Between Structure and Morphology of Crystals. I," *Acta. Cryst.*, bf 8, 49 (1955).

Hartman, P., "Crystal Form and Crystal Structure," *Physics and Chemistry of the Organic Solid State*, D. Fox, M. M. Labes, and A. Weissberger, eds., Wiley, New York (1963).

Herring, C., "Some Theorems on the Free Energies of Crystal Surfaces," *Phys. Rev.*, **82**, 87 (1951).

Herring, C., "The Use of Classical Macroscopic Concepts in Surface Energy Problems," *Structure and Properties of Solid Surfaces*, R. Gomer and C. S. Smith, eds., University of Chicago Press, Chicago (1953).

Hoffman, D. W., and J. W. Cahn, "A Vector Thermodynamics for Anisotropic Surfaces," *Surf. Sci.*, **31**, 389 (1972).

Housty, J., and M. Hospital, "Localisation des Atomes d'Hydrogène dans l'Acide Adipique," *Acta Cryst.*, **18**, 693 (1965).

Jackson, K. A., "Mechanism of Growth," *Liquid Metals and Solidification*, American Society for Metals, Cleveland (1958).

Jetten, L. A. M. J., H. J. Hunan, P. Bennema, and J. P. van der Eerden, "On the Observation of the Roughening Transition of Organic Crystals Growing from Solution," *J. Crystal Growth*, **68**, 503 (1984).

John, F., *Partial Differential Equations*, 2nd ed., Springer, New York (1975).

Kaelble, D. H., *Physical Chemistry of Adhesion*, Wiley-Interscience, New York (1971).

Kaichew, R., and I. N. Stranski, "Zur Theorie der linearen Kristallisationsgeschwindigkeit," *Z. Phys. Chem.*, **A170**, 295 (1934).

Karger, B. L., L. R. Snyder, and C. Eon, "An Expanded Solubility Parameter Treatment for Classification and Use of Chromatographic Solvents and Adsorbents," *J. Chromatography*, **125** 89 (1976).

Kitaigorodsky, A. I., K. V. Mirskaya, and A. B. Tovbis, "Lattice En-

ergy of Crystalline Benzene in the Atom-Atom Approximation,'' *Sov. Phys. Cryst.*, bf 13, 176 (1968).
Kitaigorodsky, A. I., *Molecular Crystals and Molecules*, Academic Press, New York (1973).
Klug, D. L., and J. H. van Mil, ''Adipic Acid Purification,'' United States Patent Number 5,296,639 (1994).
Koolman, H. C., and R. W. Rousseau, ''Effects of Isomorphic Compounds on the Purity and Morphology of L-Isoleucine Crystals,'' *AIChE J.*, **42**, 147 (1996).
Lahav, M., and L. Leiserowitz, ''Tailor-Made Auxiliaries for the Control of Nucleation, Growth and Dissolution of Two- and Three-Dimensional Crystals,'' *J. Phys. D*, **26**, B22 (1993).
Land, T. A., A. J. Malkin, Yu. G. Kutzensov, A. McPherson, and J. J. DeYoreo, ''Mechanism of Protein and Virus Crystal Growth: An Atomic Force Microscopy Study of Canavalin and STMV Crystallization,'' *J. Crystal Growth*, **166**, 893 (1996).
Lewis, B., ''The Growth of Crystals of Low Supersaturation, II. Comparison with Experiment,'' *J. Crystal Growth*, **21**, 40 (1974).
Lifson, S., A. T. Habler, and P. Dauber, ''Consistent Force Field Studies of Intermolecular Forces in Hydrogen-Bonded Crystals. 1.,'' *J. Am. Chem. Soc.*, bf 101, 5111 (1979).
Liu, X. Y., and P. Bennema, ''Self-Consistent Field Calculation of Structures and Static Properties of the Solid-Fluid Interface; Paraffinlike Molecule Systems,'' *Phys. Rev. E*, **48**, 2006 (1993a).
Liu, X. Y., and P. Bennema, ''The Relationship Between Macroscopic Quantities and the Solid-Fluid Interfacial Structure,'' *J. Chem. Phys.*, **98**, 5863 (1993b).
Liu, X. Y., and P. Bennema, ''Morphology of Crystal: Internal and External Habit Controlling Factors,'' *Phys. Rev. B*, **49**, 765 (1994).
Liu, X. Y., E. S. Boek, W. J. Briels, and P. Bennema, ''Prediction of Crystal Growth Morphology Based on Structural Analysis of the Solid-Fluid Interface,'' *Nature*, **374**, 342 (1995).
Liu, X. Y., and P. Bennema, ''Theoretical Consideration of the Growth Morphology of Crystals,'' *Phys. Rev. B*, **53**, 2314 (1996a).
Liu, X. Y., and P. Bennema, ''An Inhomogeneous Cell Model and the Growth of Crystals,'' *J. Crystal Growth*, **166**, 112 (1996b).
Liu, X. Y., and P. Bennema, ''Growth Morphology of Crystals and the Influence of Fluid Phase,'' *Crystal Growth of Organic Materials*, A. S. Myerson, D. A. Green, and P. Meenan, eds., ACS, Washington (1996c).
Manne, S., J. P. Cleveland, G. D. Stucky, and P. K. Hansma, ''Lattice Resolution and Solution Kinetics and Surfaces of Amino Acid Crystals: An Atomic Force Microscopy Study,'' *J. Crystal Growth*, **130**, 133 (1993).
Mason, R., ''The Crystallography of Anthracene 95°K and 290°K,'' *Acta Cryst.*, **17**, 547 (1964).
Markov, I. V., *Crystal Growth for Beginners*, World Scientific, Singapore (1995).
Mayo, S. L., B. D. Olafson, and W. A. Goddard, III, ''DREIDING: A Generic Force Field for Molecular Simulations,'' *J. Phys. Chem.*, **94**, 8897 (1990).
McConnell, J. F., ''2-(4-Isobutylphenyl) Propionic Acid,'' *Cryst. Struct. Comm.*, **3**, 73 (1974).
Michaels, A. S., and A. R. Colville, Jr., ''The Effect of Surface Active Agents on Crystal Growth Rate and Crystal Habit,'' *J. Phys. Chem.*, **64**, 13 (1960).
Momany, F. A., L. M. Curuthers, R. F. McGuire, and H. A. Scheraga, ''Intermolecular Potentials from Crystal Data,'' *J. Phys. Chem.*, **78**, 1595 (1974).
Myerson, A. S., and M. Saska, ''Calculation of Crystal Habit and Solvent-Accessible Areas of Sucrose and Adipic Acid Crystals,'' *Crystallization as a Separations Process*, A. S. Myerson and K. Toyokura, eds., ACS, Washington (1990).
Myerson, A. S., and R. Ginde, ''Crystals, Crystal Growth, and Nucleation,'' *Handbook of Crystal Growth*, A. S. Myerson, ed., Butterworth-Heinemann, Boston (1993).
Ohara, M., and R. C. Reid, *Modeling Crystal Growth Rates from Solution*, Prentice-Hall, Englewood Cliffs, NJ (1973).
Pfefer, G., and R. Boistelle, ''Control of Molecular Crystal Morphology,'' *Trans. IChemE.*, **74**, 744 (1996).
Reynolds, G. F., ''Crystal Growth,'' *Physics and Chemistry of the Organic Solid State*, D. Fox, M. M. Labes, and A. Weissberger, eds., Wiley, New York (1963).
Romero, A. J., G. Lucas, and C. T. Rhodes, ''Influence of Different Sources on the Processing and Biopharamaceutical Properties of High-dose Ibuprofen Formulations,'' *Pharm. Acta Helv.*, **66**, 34 (1991).
Sandler, S. I., *Chemical and Engineering Thermodynamics*, 2nd ed., Wiley, New York (1989).
Saska, M., and A. S. Myerson, ''The Theoretical Shape of Sucrose Crystals from Solution,'' *J. Crystal Growth*, **61**, 546 (1983).
Schwinn, T., H. E. Gaub, and J. P. Rabe, ''Supramolecular Structures and Dynamics of Organic Adsorbate Layers at the Solid-Liquid Interface,'' *Supramolecul Sci.*, **1**, **85** (1994).
Storey, R. A., ''The Nucleation, Growth and Solid-State Properties of Particulate Pharmaceuticals,'' Ph.D. Thesis, University of Bradford, U.K. (1997).
Swendson, R. H., P. J. Kortman, D. P. Landau, and H. Muller-Krumbhaar, ''Spiral Growth of Crystals: Simulation on a Stochastic Model,'' *J. Crystal Growth*, **35**, 73 (1976).
Tanguy, D., and P. Marchal, ''Relations between the Properties of Particles and their Process of Manufacture,'' *Trans IChemE*, **74**, 715 (1996).
Tavare, N. S., *Industrial Crystallization*, Plenum, New York (1994).
Taylor, J. E., ''Crystalline Variational Problems,'' *Bull. Am. Math. Soc.*, **84**, 568 (1978).
Taylor, J. E., J. W. Cahn, and C. A. Handwerker, ''I—Geometric Models of Crystal Growth,'' *Acta. Metall. Mater.*, **40**, 1443 (1992).
Volmer, M., and M. Marder, ''Zur Theorie der linearen Kristallisations-geschwindigkeit unterkuhlter Schemlzen und unterkuhlter fester Modifikationen,'' *Z. Phys. Chem.*, **A154**, 97 (1931).
Walker, E., and K. J. Roberts, *Molecular Simulations Application Notes, CGR 10*, Biosym/Molecular Simulations Inc. (1993).
Wells, A. F., ''Crystal Habit and Internal Structures—I,'' *Phil. Mag.*, **37**, 184 (1946).
Wells, A. F., ''Crystal Growth and Chemical Structure,'' *Structure and Properties of Solid Surfaces*, R. Gomer and C. S. Smith, eds., University of Chicago Press, Chicago (1953).
Williams, D. E., ''Nonbonded Potential Parameters Derived from Crystalline Aromatic Hydrocarbons,'' *J. Chem. Phys.*, **45**, 3770 (1966).
Winn, D., and M. F. Doherty, ''A New Technique for Predicting the Shape of Solution-Grown Organic Crystals,'' *AIChE J.*, **44**, 2501 (1998).
Winn, D., and M. F. Doherty, ''Predicting the Shape of Organic Crystals Grown from Polar Solvents,'' *Proc. of the 14th Int. Symp. on Ind. Crystallization*, Institution of Chemical Engineers, London, U.K. (1999).
Wulff, G., ''Zur Frage der Geschwindigkeit des Wachsthums und der Auflösung der Krystallflächen,'' *Z. Kryst.*, **34**, 449 (1901).
Yip, C. M., and M. D. Ward, ''Atomic Force Microscopy of Insulin Single Crystal: Direct Visualization of Molecules and Crystal Growth,'' *Biophys. J.*, **71**, 1071 (1996).
York, P., ''Solid-State Properties of Powders in the Formulation and Processing of Solid Dose Forms,'' *Int. J. Pharm.*, **14**, 1071 (1983).

Appendix

Liu and Bennema interpretation of the BCF/Chernov model

The pioneering work of Burton, Cabrera, and Frank (1951) is the most well known model of the growth of material on a crystal surface. The basic premise is that a flat face grows by the lateral movement of steps across the face. If the velocity of the lateral movement is v, the height of each step h, and the distance between steps y_o, then the rate of growth normal to the face is given by

$$R = v \times h/y \tag{A1}$$

The BCF mechanism requires a source of steps. Under the moderate supersaturation with which most materials will crystallize, the most likely source of steps are screw dislocation. Growth from these sites leads to spirals of steps that

propagate continuously while spreading laterally. There is substantial experimental evidence that crystal faces grow by the advancement of spirals (Reynolds, 1963; Land et al., 1996).

The distance between steps on a spiral y is just the distance between the turns of the spiral. This measure is related to the geometry of a 2-D nucleus. Bennema and Liu employ the result of Cabrera and Levine (1956) who gave the distance between turns as approximately $19r_c$, where r_c is the critical radius of a 2-D nucleus (see Ohara and Reid, 1973, for the derivation of this relationship). The critical nucleus radius is given by the well known formula:

$$r_c = V_m \gamma^{\text{step}} / \Delta\mu \tag{A2}$$

The critical size for the existence of a 2-D nucleus, a disk of lattice spacing thickness, can be derived as follows: When solute from a supersaturated solution transforms into a crystalline 2-D nucleus, the total Gibbs free energy of the system increases as a new surface is formed, but decreases as material goes from higher to lower chemical potential. This leads to a maximum in the Gibbs energy at some critical size of the new solid. The free energy change is $\Delta G = -N\Delta\mu + \gamma A$, where the first term represents the decrease due to the phase change, and the second term is the increase in energy from the new surface of area A. If the nucleus is formed on an existing crystal face, then the new surface is the ''stepped'' surface—the surface of thickness d and area $2\pi rd$ wrapping around the disk. Replacing N with $\pi r^2 d/V_m$ (the volume of the disk divided by the molecular volume), the maximum in ΔG can be determined by setting its first derivative with respect to r equal to zero. Thus, the expression for the critical radius $r_c = V_m \gamma^{\text{step}}/\Delta\mu$, where γ^{step} is the specific step free energy.

In the formula $\Delta\mu = \mu - \mu_{\text{sat}}$, the difference in the chemical potentials between the solute in solution and in the crystal (in units of energy per molecule), V_m is the molecular volume, and γ_{step} is the step free energy per step area–the specific energy of forming the surface of monolayer thickness wrapping around the 2-D nucleus.

Substituting $19r_c$ for y in Eq. A1, the expression for the normal growth of a crystal face can be written as

$$R = \frac{\upsilon h \Delta\mu}{19 V_m \gamma^{\text{step}}} \tag{A3}$$

This equation has three face dependent parameters: υ, h, and γ^{step}. The step height h is assumed to be of monolayer thickness, and, hence, is approximated by the interplanar spacing d_{hkl}. (This assumption has been validated by recent AFM measurements of step heights (Manne et al., 1993; Yip and Ward, 1996)). The specific step free energy and lateral step velocity are face dependent and can be written as $\gamma^{\text{step}}_{hkl}$ and υ_{hkl}, respectively.

The specific step energy has a single value per face, dictating that the spirals, like 2-D nuclei, are completely circular. (In other words, Bennema and Liu have assumed that on any given face, the surface energy of a step is anisotropic.) However, the spirals are only approximately circular. They actually consist of many steps of finite area and orientation that approximate a circular disk. Therefore, $\gamma^{\text{step}}_{hkl}$ is an average over many step orientations, and can be expressed as

$$\gamma^{\text{step}}_{hkl} = \bar{\phi}_{hkl}/a^2 \tag{A4}$$

where $\bar{\phi}_{hkl}$ is termed *the mean step energy*: the mean surface energy per molecule on the steps. The step surface area per molecule is a^2, where a is molecular length. (The actual height, width, and depth (a_h, a_w, a_d) of these step sites (step molecules) are generally different from each other, and vary with step orientation and the face orientation. However, the molecular volume ($a_h \times a_w \times a_d$) is a constant. Since only the volume appears in the final growth rate expression, we leave off the subscripts in the development. We denote molecular length with a, area with a^2, and volume with a^3, which is equal to V_m). If we consider any molecule on the step as a *step site*, then we can refer to $\bar{\phi}$ and a^2 as the mean surface energy and surface area of a step site. Substituting this expression into Eq. A3

$$R_{hkl} = \frac{a^2 \upsilon_{hkl} d_{hkl} \Delta\mu}{19 V_m \bar{\phi}_{hkl}} \tag{A5}$$

Equation A5 is the exact expression for normal growth by the screw dislocation mechanism. Its application requires estimates of υ_{hkl} and $\bar{\phi}_{hkl}$.

Estimating lateral step velocity

Much of the work in the investigation of crystal growth has focused on the mechanisms for transport and incorporation of material at steps (see Chernov, 1984). The overall rate of step propagation is thought to be a function of one or more of the following transport processes: bulk diffusion to the surface of the crystal, surface diffusion to steps, and incorporation of material into kinks on the step. There exists two models of step growth that closely match experiments: the BCF surface diffusion model (Burton et al., 1951) (a rate expression that includes surface diffusion and incorporation), and the Chernov model (Chernov, 1984) (combining bulk diffusion and incorporation). The dependence of the overall growth rate on supersaturation described by these models closely matches the actual dependence seen experimentally. The BCF model most closely predicts vapor-phase crystal growth, while the Chernov model more closely predicts solution growth.

In the limit of very fast diffusion—and/or in the limit of a small diffusion boundary layer in the Chernov model—both models reduce to finding the rate of incorporation of solute at kinks; incorporation becomes the rate limiting step. This limit may often be reached in well mixed, solution crystallization systems. Hence, we will only explore the kinetics of solute incorporation in this section.

Bennema and Gilmer (1973) have proposed that the rate at which solute incorporates into kinks is an activated process that can be modeled using a similar statistical mechanical formalism as gas-phase collision theory (see the work of Eyring and coworkers, (Glasstone et al., 1941)). In this ap-

proach, the velocity of a step is expressed as the product of the frequency of incorporation at kinks and the distance the step is propagated; the former is just the probability of there being a kink site times the net frequency of molecules entering a kink

$$\upsilon = a\frac{a}{\lambda_0}(j_+ - j_-) \tag{A6}$$

where a is the propagation distance (molecular length), a/λ_0 is the probability of a kink (the molecular length divided by the distance between kinks), and $j_+ - j_-$ is the net frequency of entering molecules.

The frequencies of entering and leaving a kink site depend on the nature of the fluid phase. For growth from solution, they can be expressed as (Markov, 1995)

$$j_+ = \nu X_A V_m \exp\left(\frac{-E}{kT}\right)$$

$$j_- = \nu(1 - X_A V_m)\exp\left(-\frac{(\Delta H_d + E)}{kT}\right)$$

where ν is the vibrational frequency of the molecule, assumed to be the same for both entering and leaving the kink. $X_A V_m$ is the concentration of solute at the kink times the molecular volume, which is the probability of a solute molecule available for incorporation, and, hence, $(1 - X_A V_m)$ is the probability that there are solvent molecules available for solvation when solute leaves the kink. (Note that later we will write X_A as $X_{A(hkl)}$, because it is the local concentration of solute on the crystal face.) The exponential terms represent the probability of a molecule having the necessary energy for entering/leaving. For liquid to solid transitions, the necessary energy is the activation energy E for entry into a kink. For solid to liquid transitions, it is the activation energy plus the enthalpy of dissolution.

At equilibrium, both fluxes are equal ($j_+ = j_-$), and, thus

$$\exp\left(-\frac{\Delta H_d}{kT}\right) = \frac{X_A^0 V_m}{1 - X_A^0 V_m} \tag{A7}$$

where X_A^0 is the equilibrium concentration. Substituting these expressions into Eq. A6

$$\upsilon = a\frac{a}{\lambda_0}\nu\exp\left(\frac{-E}{kT}\right)\left[X_A V_m - (1 - X_A V_m)\frac{X_A^0 V_m}{1 - X_A^0 V_m}\right] \tag{A8}$$

In the case of a dilute solution, $X_A^0 V_m \ll 1$, and this expression reduces

$$\upsilon = a\frac{a}{\lambda_0}\nu\exp\left(\frac{-E}{kT}\right)V_m(X_A - X_A^0) \tag{A9}$$

It is commonly written as

$$\upsilon = \beta V_m(X_A - X_A^0) = \beta V_m X_A^0 \sigma \tag{A10}$$

where $\sigma = (X_A - X_A^0)/X_A^0$, the relative supersaturation, and $\beta = a(a/\lambda_0)\nu\exp(-E/kT)$ and is termed the kinetic coefficient of a step. (We have left off the subscript hkl on X_A and X_A^0 for clarity: they are interfacial concentrations. However, we do assume that their relative difference is not anisotropic and is equivalent to the bulk supersaturation.)

The key parameter in the above expression is β; it is the principal anisotropic parameter affecting step velocity. The anisotropy comes from the mean distance between kinks λ_0 and the activation energy for incorporation at kinks E. Both are functions of the mean work to form a kink $\overline{\phi}^{\text{kink}}$, which as shown by Liu et al. (1995), is approximately the same as the work to form a stepped surface

$$\overline{\phi}^{\text{kink}} = \overline{\phi}^{\text{step}} = \overline{\phi}$$

Hence, we can employ the BCF relationship for the distance between kinks, $\lambda_0 = a(1 + (1/2)\exp\overline{\phi}/kT)$, which in the limit of $\lambda_0 \gg a$ reduces to

$$a/\lambda_0 \approx 2\exp\left(-\overline{\phi}/kT\right) \tag{A11}$$

For the activation energy, we employ the model of Liu and Bennema (1996a). They divide the energy barrier into two contributions: the free energy of desolvation $\Delta G''$, and the free energy associated with the transition to an effective growth unit, which we will term t_{hkl}. The former is thought to be isotropic, while the latter is not. From the difference in chemical potentials, the t_{hkl} term can be approximated by $-kT\ln[X^{\text{eff}}_{A(hkl)}/X_{A(hkl)}]$. Thus, the kinetic coefficient can now be written as a function of each face

$$\beta_{hkl} = a\nu 2\exp\left(-\overline{\phi}_{hkl}/kT - t_{hkl} - \Delta G''\right) \tag{A12}$$

where $\overline{\phi}_{hkl}$ and t_{hkl} are the only unknown anisotropic parameters.

Estimating step energy

In analogy to Gibbs' definition of the surface energy, the mean step energy can be defined as the average work required to form a stepped surface. Using the *inhomogeneous cell model*, Liu and Bennema (1993b, 1996a) have derived an expression relating mean step energy to known or measurable quantities. This model of the solid-liquid interface has the following characteristics:

(1) The solid and liquid phase are divided into cells of equal shape and volume; for example, cubes.

(2) Every cell is occupied by either solid or liquid units.

(3) All of the interaction energy (van der Waals, electrostatic) for each cell is a result of only first nearest neighbor interactions. This is a reasonable assumption since in general over 85% of the lattice energy of organics comes from first nearest neighbor interactions.

Within the framework of this model, ϕ_i can be defined as the work required to form one solid-fluid contact in the i direction. it is given by

$$\phi_i = \phi_i^{sf} - \frac{1}{2}\left(\phi_i^{ss} + \phi_i^{ff}\right) \tag{A13}$$

where ϕ_i^{sf}, ϕ_i^{ss}, and ϕ_i^{ff} indicate interaction energies (bonds) between solid-fluid, solid-solid, and the fluid-fluid units, respectively. This relationship is easily derived from examining the work required to exchange one solid unit for one fluid unit in a cubic cell model: 12 solid-fluid contacts are formed by making 12 solid-fluid bonds, and breaking 6 solid-solid and 6 fluid-fluid bonds. If we further restrict ϕ_i to being the work of forming solid-fluid contacts by the molecules at a crystal-fluid interface (as opposed to those in the bulk), then for an i which is a step direction, ϕ_i is a step energy. The average over all n step directions is the mean step energy

$$\overline{\phi}_{hkl} = \frac{\sum_{i=1}^{n_{hkl}} \phi_i}{n_{hkl}} \tag{A14}$$

where n_{hkl} is the number of first nearest neighbors positioned laterally around a molecule in a slice; that is, to say, the number of first nearest neighbors in the ''slice'' direction. As well, the sum of all the work to form solid-liquid contacts is the enthalpy of dissolution per molecule

$$\Delta H_{hkl}^{\text{diss}} = \sum_{i=1}^{m} \phi_i \tag{A15}$$

where m is the total number of first nearest neighbor bonds.

Note that Eq. A15 defines an enthalpy of dissolution of material in a surface region, at a face *hkl*. It has a different value on different crystal faces, a result of the fact that ϕ_i is itself anisotropic. This is one of the primary features of the inhomogeneous cell model: the crystal surface has macroscopic properties, such as enthalpy, that are different than those in the bulk. This insight is consistent with experimental studies of surface roughening (also known as surface melting). At a temperature below the melting point, flat facets may roughen as a result of a local phase transition. A discussion of the existence of surface roughening and face specific enthalpy can be found in the work of Jackson (1958) and Bennema and Gilmer (1973).

In order to express $\overline{\phi}_{hkl}$ is terms of measurable quantities, one more assumption is applied to the binding energies: the so-called *proportionality condition* (Liu and Bennema, 1994). It assumes that the ratio of interactions in any two directions in one phase (such as the bulk crystal) is the same as that for another phase (such as the surface phase). It is expressed as

$$\phi_i : \phi_j = \Phi_i : \Phi_j$$

where i and j are directions, and Φ_i represents the same work as ϕ_i except that it is for molecules in the bulk crystal. Recalling the lattice and slice energies, properties of the bulk crystal can be defined in terms of the cell model (since E^{latt} represents the work of formation from a vacuum, Φ_i^{sf} and Φ_i^{ff} are zero, and, hence, $E^{\text{latt}} = \sum_{i=1}^{m} 1/2\Phi^{ss}$. This expression for the lattice energy is consistent with the calculation in the attachment energy model.)

$$E^{\text{latt}} = \sum_{i=1}^{m} \Phi_i$$

$$E_{hkl}^{sl} = \sum_{i=1}^{n_{hkl}} \Phi_i$$

we can compare them to the surface properties by means of the proportionality condition

$$\frac{\overline{\phi}_{hkl} n_{hkl}}{\Delta H_{hkl}^{\text{diss}}} = \frac{E_{hkl}^{sl}}{E^{\text{latt}}} \tag{A16}$$

The term $\overline{\phi}_{hkl} n_{hkl}$ can be thought of as the surface slice energy, or in other words, the average in-plane contribution to the enthalpy of dissolution of the face. Rearranging Eq. A16, and defining $E_{hkl}^{sl}/E^{\text{latt}}$ as ξ_{hkl}, we can express the mean step energy as

$$\overline{\phi}_{hkl} = \xi_{hkl} \Delta H_{hkl}^{\text{diss}} / n_{hkl} \tag{A17}$$

Using classical solubility thermodynamics, it is possible to develop an expression that relates the enthalpy of dissolution to saturation concentration in solution. (Since the partial molar Gibbs energy of fusion ΔG^f is non-zero for temperatures below the melting point at which solute dissolves in solution, we can write (see Sandler, 1989) $-\Delta G^f = RT \ln \gamma_A X_A^0$, where γ_A is the activity coefficient and X_A^0 is the saturation concentration. Also $\Delta G^f = \Delta H^f - T\Delta S^f$, where the changes in entropy and enthalpy are at the system temperature T. Recalling that $\Delta H^f(T^m) = T^m \Delta S^f(T^m)$, and ignoring the variation of enthalpy and entropy with temperature, we can write $RT \ln \gamma_A X_A^0 = -\Delta H^f(1 - T/T^m)$. Since $RT \ln \gamma_A = G^{\text{EX}}$, then for a regular solution where $S^{\text{EX}} = 0$, $RT \ln \gamma_A = \Delta H^{\text{mix}}$. Defining the enthalpy of dissolution as the sum of the enthalpies of mixing and fusion, we now have $\ln X_A^0 = -\Delta H^{\text{diss}}/RT + \Delta H^f/RT^m$. For an ideal liquid mixture, or one close to ideal where ΔH^{mix} is small, we can write $\ln X_A^0 \approx \Delta H^{\text{diss}}(T - T^m)/RTT^m$.) It is sometimes termed the van't Hoff equation (Liu and Bennema, 1993b), and be applied to both bulk and surface properties

$$\ln X_A^0 \approx \Delta H^{\text{diss}}(T - T^{\text{melt}})/kTT^{\text{melt}} \tag{A18}$$

$$\ln X_{A(hkl)}^{0(\text{eff})} \approx \Delta H_{hkl}^{\text{diss}}(T - T^{\text{melt}})/kTT^{\text{melt}} \tag{A19}$$

where X_A^0 is the equilibrium concentration of solute in bulk solution at a given T, and $X_{A(\text{hkl})}^{0(\text{eff})}$ is the local concentration of effective growth units near the crystal face. The existence of this local concentration of solute has been suggested by both computational and experimental interface studies (Schwinn et al., 1994; Curry and Cushman, 1995). The ''effective'' growth units are those in the adsorbed layer whose orientation and conformation allow them to effectively participate in dynamic equilibrium with the molecules at the crystal surface. (See Liu and Bennema (1993b) for further discussion of effective growth units.) For structurally simple molecules, $X_{A(hkl)}^{\text{eff}} \cong X_{A(\text{hkl})}$, which is just the total concentration of local growth units. Either quantity can be estimated from molecular modeling of solute and solvent in contact with the crystal face such as molecular dynamics (Boek et al., 1994) and self-consistent field methods (Liu and Bennema, 1993a). There-

fore, the mean step energy can be completely defined as a function of measurable and/or known quantities

$$\bar{\phi}_{hkl} = \xi_{hkl} C_{hkl} \Delta H^{\text{diss}} / n_{hkl} \tag{A20}$$

where C_{hkl} is termed the surface scaling factor

$$C_{hkl} = \frac{\Delta H^{\text{diss}}_{hkl}}{\Delta H^{\text{diss}}} = \frac{\ln X^{0(eff)}_{A(hkl)}}{\ln X^{0}_{A}} \tag{A21}$$

It is possible to directly estimate $\Delta H^{\text{diss}}_{\text{hkl}}$, and, hence, C_{hkl}, from experimental measurements of the surface roughening temperature (Liu and Bennema, 1996c). If the data are not available, molecular modeling must be implemented to measure C_{hkl}. In the case where $C_{hkl} = 1$, the adlayer has the same composition as the bulk solution, and the surface thermodynamic properties are the same as those of the bulk crystal. This is known as the *equivalent wetting* condition: no effect of the solvent on the surface properties, and, hence, no effect on the growth rate. This is unlikely to occur in practice; the deviation of C_{hkl} from unity is what distinguishes the effect of one solvent from another on the crystal shape.

Complete growth rate expression

Combining the equations for the normal growth rate, the lateral step velocity, the kinetic coefficient, and the mean step energy (Eqs. A5, A10, A12, and A20), we can write

$$R_{hkl} = \frac{2\nu d_{hkl} V_m X^{0}_{A(hkl)} \sigma^2}{19 \xi_{hkl} C_{hkl} \epsilon / n_{hkl}} \exp\left(-\xi_{hkl} C_{hkl} \epsilon / n_{hkl} - t_{hkl} - \Delta G''\right) \tag{A22}$$

where $\epsilon = \Delta H^{\text{diss}} / kT$. Leaving only the face dependent parameters

$$R_{hkl} \propto d_{hkl} n_{hkl} \left[X^{0}_{A} \right]^{C_{hkl}} \left(\xi_{hkl} C_{hkl} \right)^{-1} \exp\left(-\xi_{hkl} C_{hkl} \epsilon / n_{hkl}\right) \tag{A23}$$

Using values of d_{hkl} and ξ_{hkl} from BFDH and attachment energy calculations, along with n_{hkl} from visual examination of the slice structure, and C_{hkl} from solid-fluid interface modeling, we can estimate the relative growth rates and shape of solution grown crystals.

Manuscript received Jan. 12, 1999, and revision received Feb. 17, 2000.